COST Action 18232
Mathematical Models for Interacting Dynamics on Networks
WG 5: Numerical Methods and Applications
– White Paper –

Dynamics of and on networks: Numerics, control, applications

Sílvia Barbeiro[1], Petra Csomós[2,3], Matthias Ehrhardt[4], Jan Giesselmann[5], Martin Gugat[6], Peter Kogut[7], Teresa Kunkel[5], Ivica Nakić[8], Josip Tambača[9], Zoran Tomljanović[10], Hamdullah Yücel[11], Enrique Zuazua[6,12,13]

March 2024

Preface

Many physical, biological, chemical, financial, and social phenomena can be described by dynamical systems and frequently the dynamics are coupled in a networked structure. The nature of these connections can be quite different, ranging from situations where connections express interactions between certain agents in multi-agent systems to situations where connections are gas pipes in gas transport networks.

Very often the differential equations arising in applications have a rather complex structure so that analytical solution formulas are not available; in this case, numerical simulations are a natural tool to gain insights into the solution behavior.

Working Group 5: Numerical Methods and Applications of COST Action 18232 brought together experts from different fields of mathematics in order to devise and analyse novel numerical schemes for networked dynamics. This took place in close cooperation with the more analysis-driven investigations in other working groups.

Due to the different natures of the studied applications the resultant models displayed a variety of mathematical structures. Thus, different problem-adapted numerical schemes needed to be developed and different techniques needed to be used for their analysis. With an eye towards providing suitable tools for different applications the working group members applied methods from such diverse fields of mathematics as numerical analysis, control theory, semi-group theory, and homogenization.

The following white paper showcases progress made by the members of the working group in the last years and relates it to the state of the art in the corresponding areas.

Chapter 1

Numerical Methods for Networked PDEs

1.1 Wave Dynamics in Quantum Networks with Transparent Branching Points

In this section various applications of absorbing boundary conditions in different physical scenarios are discussed, emphasizing their use in modeling reflectionless transport phenomena for different types of solitons and particles.

The work discussed below considers the wave dynamics in quantum networks with transparent branching points. The latter means that the transmission of waves/particles through the vertices of the network occurs without reflection. This is done by solving linear and nonlinear Schrödinger equations on metric graphs, for which so-called absorbing vertex boundary conditions are imposed at the graph vertices to ensure the transparency of the network. Applications of the results to the modelling and design of various optical fibre networks and branched nanoscale systems are briefly discussed.

Absorbing boundary conditions at branching points in networks

Quantum graphs have been shown to be accurate models for the study of quantum transport and spectral statistics in nanoscale systems. Recently, such graphs have been studied experimentally using microwave networks consisting of coaxial waveguides. Zero point energy in quantum graphs can play an important role in various systems (e.g. polymers, molecular networks, microwave networks and other supramolecular structures) whose dynamics can be modelled by quantum graphs, as well as in nanomechanics.

The problem of absorbing boundary conditions (ABCs) for wave equations has attracted much attention in several practically important contexts. Such boundary conditions are commonly considered when investigating two processes: the absorption of particles and waves as they pass from one domain to another, and the reflectionless transmission of particles (waves) through the boundary of a given domain.

In general, ABCs can be derived by factorizing the differential operator corresponding to a wave equation. However, this often leads to a form for the boundary conditions which is much more complicated than that of the Dirichlet, Neumann and Robin conditions. In addition, when complemented with ABCs, the wave equation cannot be solved analytically and always requires the use of numerical methods. The choice of discretisation scheme depends on both the type of wave equation and the type of process.

The following discussion concerns the application of absorbing boundary conditions to quantum graphs, considering the problem of reflectionless transmission of the particle through the vertex of the graph. In particular, the objective is the extension of the classical derivation of ABCs for Schrödinger equations first to the case of star-shaped graphs, then to more general quantum graphs.

The state of the art

The state of the art in applying absorbing boundary conditions [6, 10] to solve wave equations on quantum networks modeled as metric graphs [94], can be summarised as follows.

Quantum graphs are established models for studying wave phenomena in nanoscale systems like optical fibers and microwave networks. The research focuses on developing ABCs for these networks to ensure reflectionless transmission of waves/particles through branching points (vertices) of the graph. The study uses the linear and nonlinear Schrödinger equations on these graphs. Classical ABC derivations for Schrödinger equations are being extended to quantum graphs. Thus the idea is to begin with the simplest case of the star-shaped graph.

The derivation of ABCs is an important step towards solving numerically wave dynamics in complex quantum networks with minimal reflection at branching points, which is crucial for accurate simulations in various applications such as the designing of optical fibers and nanoscale systems.

Driven transparent quantum graph

In the work [142], the authors discuss the concept of quantum graphs with transparent vertices by considering the case where the graph interacts with an external time-independent field. In particular, the problem of absorbing boundary conditions for quantum graphs is addressed, building on previous work on absorbing boundary conditions for the stationary Schrödinger equation on a line. Physically relevant constraints making the vertex transparent under boundary conditions in the form of (weight) continuity and Kirchhoff rules are derived using two methods, the scattering approach and absorbing boundary conditions for the time-independent Schrödinger equation. The latter is derived by extending the absorbing boundary condition concept to the time-independent Schrödinger equation on driven quantum graphs. Further, the authors consider how the eigenvalues and eigenfunctions of a quantum graph are influenced not only by its topology, but also by the shape/type of a potential when an external field is involved.

The scattering approach

The concept of absorbing boundary conditions has recently been extended to the case of evolution equations on graphs, by considering linear [141] and nonlinear [140] Schrödinger equations on graphs and the Dirac equation on quantum graphs [139]. In all cases the focus was on time-dependent equations.

In [142] the authors instead consider the stationary Schrödinger equation on the star graph with some potential $V_j(x)$ given on each of its bonds (edges) j :

$$-\frac{\mathrm{d}^2}{\mathrm{d}x^2}\Psi_j(x) + V_j(x)\Psi_j(x) = k^2\Psi_j(x), \quad j = 1, 2, \ldots, N,$$

One of the boundary conditions at the vertex can be written as a generalized form of the continuity condition

$$\alpha_1\Psi_1(0) = \alpha_2\Psi_2(0) = \ldots = \alpha_N\Psi_N(0), \tag{1.1}$$

and the current conservation

$$\sum_{j=1}^{N} \frac{1}{\alpha_j}\frac{\mathrm{d}}{\mathrm{d}x}\Psi_j(0) = 0, \tag{1.2}$$

where $\alpha_j \in \mathbb{R}$ are some non-zero coefficients.

In this case, the components $\Psi_{i,j}(x)$ of the total wave function can be written as

$$\Psi_{i,j}(x) = \delta_{j,i}\, \mathrm{e}^{-\mathrm{i}\sqrt{k^2-V_j(x)}x} + \sigma_{i,j}\, \mathrm{e}^{\mathrm{i}\sqrt{k^2-V_j(x)}x}. \tag{1.3}$$

The boundary conditions (1.1) and (1.2) at the vertex together with (1.3) can be used to determine $\sigma_{i,i}$

$$\sigma_{i,i} = \frac{1 - \sum\limits_{\substack{j=1 \\ j\neq i}}^{N} \frac{\alpha_i^2}{\alpha_j^2} \sqrt{\frac{k^2-V_j(0)}{k^2-V_i(0)}}}{1 + \sum\limits_{\substack{j=1 \\ j\neq i}}^{N} \frac{\alpha_i^2}{\alpha_j^2} \sqrt{\frac{k^2-V_j(0)}{k^2-V_i(0)}}}.$$

Requiring the reflection probability to be equal to zero yields the energy dependent expression

$$\frac{\sqrt{k^2 - V_i(0)}}{\alpha_i^2} = \sum_{\substack{j=1 \\ j\neq i}}^{N} \frac{\sqrt{k^2 - V_j(0)}}{\alpha_j^2}.$$

The condition that all the bond potentials have the same value at the vertex (i.e. $V_1(0) = V_2(0) = \cdots = V_N(0)$) determines a constraint given by a sum rule

$$\frac{1}{\alpha_i^2} = \sum_{\substack{j=1 \\ j\neq i}}^{N} \frac{1}{\alpha_j^2}.$$

Finally, it is also shown in [142] that one can also derive this sum rule using the concept of ABCs to derive the conditions for the vertex transparency.

ABCs for the nonlocal nonlinear Schrödinger equation

The work [1] considers the problem of reflectionless propagation of parity-time-symmetric (PT-symmetric) solitons described by the nonlocal nonlinear Schrödinger equation on a line in the framework of the concept of absorbing boundary conditions (ABCs) for evolution equations. ABCs for the nonlocal nonlinear Schrödinger equation are also derived. The absence of backscattering at the artificial boundaries is confirmed by the numerical implementation of the absorbing boundary conditions.

The nonlocal nonlinear Schrödinger (NNLS) equation is

$$\mathrm{i}\partial_t q(x,t) + \partial_{xx} q(x,t) + 2q(x,t)q^*(-x,t)q(x,t) = 0. \tag{1.4}$$

To derive ABCs for the NNLS equation (1.4), the authors of [1] use the so-called *potential approach* which was previously applied to derive ABCs for coupled nonlinear Schrödinger equations [120]. This allows for the formal reduction of the NNLS equation (1.4) to the linear Schrödinger equation

$$\mathrm{i}\partial_t q(x,t) + \partial_{xx} q(x,t) + V(x,t)q(x,t) = 0,$$

with the potential $V(x,t) = 2q(x,t)q^*(-x,t)$.

The authors proceed by introducing a new unknown $Q(x,t)$, which is given by the relation

$$Q(x,t) = \mathrm{e}^{-\mathrm{i}\mathcal{V}(x,t)}\, q(x,t), \qquad \mathcal{V}(x,t) = \int_0^t V(x,s)\,\mathrm{d}s.$$

The temporal and spatial derivatives of q can be written as derivatives of Q as

$$\partial_t q = \mathrm{e}^{\mathrm{i}\mathcal{V}}(\partial_t + \mathrm{i}V)Q, \tag{1.5}$$

and

$$\partial_{xx} q = \mathrm{i}\mathrm{e}^{\mathrm{i}\mathcal{V}}(\partial_{xx}Q + 2\mathrm{i}\partial_x\mathcal{V}\partial_x Q + \mathrm{i}Q\partial_{xx}\mathcal{V} - (\partial_x\mathcal{V})^2 Q). \tag{1.6}$$

Thus the Schrödinger equation in terms of $Q(x,t)$ is

$$L(x,t,\partial_x,\partial_t)Q := \mathrm{i}\partial_t Q + \partial_x^2 Q + A\partial_x Q + BQ = 0, \tag{1.7}$$

where $A = 2\mathrm{i}\partial_x\mathcal{V}$ and $B = (\mathrm{i}\partial_{xx}\mathcal{V} - (\partial_x\mathcal{V})^2)$. Using the pseudo-differential operator calculus, equation (1.7) can be linearized with

$$L = (\partial_x + \mathrm{i}\Lambda^-)(\partial_x + \mathrm{i}\Lambda^+) = \partial_x^2 + \mathrm{i}(\Lambda^+ + \Lambda_-)\partial_x + \mathrm{i}\,\mathrm{Op}(\partial_x\lambda^+) - \Lambda^+\Lambda^-, \tag{1.8}$$

where λ^+ is the principal symbol of the operator Λ^+ and $\mathrm{Op}(p)$ denotes the associated operator of a symbol p. The equations (1.7) and (1.8) lead to the system of operators

$$\begin{aligned}
&\mathrm{i}(\Lambda^+ + \Lambda^-) = A,\\
&\mathrm{i}\,\mathrm{Op}(\partial_x\lambda^+) - \Lambda^+\Lambda^- = \mathrm{i}\partial_t + B.
\end{aligned}$$

An asymptotic evolution in the inhomogeneous symbols can be written as

$$\lambda^\pm \sim \sum_{j=0}^{+\infty} \lambda^\pm_{1/2-j/2},$$

which, following some calculation, yields the first-order approximation

$$\begin{aligned}
&\partial_x q|_{x=-L} - \mathrm{e}^{-\mathrm{i}\frac{\pi}{4}}\mathrm{e}^{\mathrm{i}\mathcal{V}}\partial_t^{1/2}(\mathrm{e}^{-\mathrm{i}\mathcal{V}}q)\big|_{x=-L} = 0,\\
&\partial_x q|_{x=L} + \mathrm{e}^{-\mathrm{i}\frac{\pi}{4}}\mathrm{e}^{\mathrm{i}\mathcal{V}}\partial_t^{1/2}(\mathrm{e}^{-\mathrm{i}\mathcal{V}}q)\big|_{x=L} = 0,
\end{aligned}$$

and the second-order approximation

$$\begin{aligned}
&\partial_x q|_{x=-L} - \mathrm{e}^{-\mathrm{i}\frac{\pi}{4}}\mathrm{e}^{\mathrm{i}\mathcal{V}}\partial_t^{1/2}(\mathrm{e}^{-\mathrm{i}\mathcal{V}}q)\big|_{x=-L} - \mathrm{i}\frac{\partial_x V}{4}\mathrm{e}^{\mathrm{i}\mathcal{V}} I_t(\mathrm{e}^{-\mathrm{i}\mathcal{V}}q)\big|_{x=-L} = 0,\\
&\partial_x q|_{x=L} + \mathrm{e}^{-\mathrm{i}\frac{\pi}{4}}\mathrm{e}^{\mathrm{i}\mathcal{V}}\partial_t^{1/2}(\mathrm{e}^{-\mathrm{i}\mathcal{V}}q)\big|_{x=L} + \mathrm{i}\frac{\partial_x V}{4}\mathrm{e}^{\mathrm{i}\mathcal{V}} I_t(\mathrm{e}^{-\mathrm{i}\mathcal{V}}q)\big|_{x=L} = 0.
\end{aligned}$$

Recall that the operator $\partial_t^{1/2}$, which denotes the half order fractional time derivative operator, is defined as

$$\partial_t^{1/2} f(t) = \frac{1}{\sqrt{\pi}}\partial_t \int_0^t \frac{f(s)}{\sqrt{t-s}}\,\mathrm{d}s,$$

and the operator $I_t(f)$ reads

$$\big(I_t(f)\big)(t) = \int_0^t f(s)\,\mathrm{d}s.$$

1.2 Numerical Solutions to Boundary Coupled Problems

Boundary coupled problems arise naturally in the mathematical description of applications where different physical/biological/etc. processes take place inside and on the boundary of a (e.g. spatial) domain. Then the solution of the differential equation posed on the boundary implies a boundary condition for the problem inside the domain. An example is the modelling the osmosis of a cell.

A particularly important field nowadays is the analysis of dynamical networks and their numerical treatment. As will be shown at the end of the section, dynamical network processes can also be written in the form of boundary coupled problems. Although there is an extensive literature treating the well-posedness, spectral properties, long time behaviour, and controllability of diffusion and/or wave equations on networks (see e.g. [43, 55, 87, 88]), the research of their numerical analysis is very incomplete. This section describes recent progress on the numerical treatment of dynamical networks in an abstract setting by using functional analytic tools.

The abstract framework of boundary coupled problems also applies to other contexts, including boundary feedback problems with bulk and boundary equations (see e.g. [23, 39, 40]), dynamic boundary conditions (see e.g. [54, 86, 135]), and diffusion processes on networks with boundary conditions satisfying ordinary differential equations in the vertices (see e.g. [107, 108, 123]).

The novelty of the approach described in this section is the application of operator splitting (similar to the bulk–surface splitting in [86]) together with an auxiliary step which has been missing from the "naive" algorithm presented in the literature before. This makes it possible to achieve the expected convergence order. In what follows the results of the publications [35] and [36] are generalized, which were carried out in the framework of the COST Action Mat-Dyn-Net.

Abstract setting

Let $(X, \|\cdot\|_X)$ and $(Y, \|\cdot\|_Y)$ be Banach spaces over $\mathbb{C}$ or $\mathbb{R}$, and consider the following operators.

Assumptions 1.2.1. *(i)* $A\colon D(A) \subset X \to X$ *and* $B\colon D(B) \subset Y \to Y$ *are linear and invertible.*

(ii) $L\colon D(A) \to Y$ *is linear, surjective, and bounded on* $D(A)$ *with respect to the graph norm of* A*,*

(iii) $\binom{A}{L}\colon D(A) \to X \times Y$ *is closed,*

(iv) $A_0 := A|_{\ker(L)}$ *is invertible and generates an analytic semigroup,*

(v) $D_0 := L|^{-1}_{\ker(A)}\colon Y \to \ker(A) \subset X$ *is called the abstract Dirichlet operator (which exists under these assumptions),*

(vi) $Q(t) = D_0 \mathrm{e}^{tB} - \mathrm{e}^{tA_0} D_0 + Q_0(t)$, $Q_0(t)y := -\int_0^t \mathrm{e}^{(t-s)A_0} D_0 \mathrm{e}^{tB} By \,\mathrm{d}s$, $y \in D(B)$, *and* $Q(t) \in \mathcal{L}(Y, X)$ *for all* $t \geq 0$*, moreover,* $\limsup\limits_{t \to 0+} \|Q(t)\| < \infty$*,*

(vii) $\mathcal{F} := (\mathcal{F}_1, \mathcal{F}_2)\colon \mathcal{D} \to X \times Y$ *is Lipschitz continuous on the set*

$$\mathcal{S} := \big\{ v \in X \times Y \colon \|(x(t), y(t)) - v\| \leq R \text{ for some } t \in [0, T] \big\} \subseteq \mathcal{D} \tag{1.9}$$

such that $\mathcal{F}_2\colon \mathcal{S} \to D(B)$ *is Lipschitz continuous and* $\mathcal{F}_2(x(t), y(t)) \in D(B^2)$ *for all* $t \in [0, T]$*, moreover,* $\sup\limits_{t \in [0,T]} \|B^2 \mathcal{F}_2((x(t), y(t))\| < \infty$*.*

Then for any given elements $x_0 \in X$ and $y_0 \in Y$, the boundary coupled problem for the unknown functions $x\colon [0,\infty) \to X$ and $y\colon [0,\infty) \to Y$ takes the following form:

$$\begin{cases} \frac{\mathrm{d}}{\mathrm{d}t}x(t) = Ax(t) + \mathcal{F}_1\big(x(t), y(t)\big), \ t \geq 0, & x(0) = x_0 \in X, \\ \frac{\mathrm{d}}{\mathrm{d}t}y(t) = By(t) + \mathcal{F}_2\big(x(t), y(t)\big), \ t \geq 0, & y(0) = y_0 \in Y, \\ Lx(t) = y(t), \ t \geq 0. \end{cases} \tag{1.10}$$

As an example one can think of a diffusion process inside and on the boundary of the bounded (spatial) domain $\Omega \subset \mathbb{R}^d$, when $X = \mathrm{L}^2(\Omega)$, $Y = \mathrm{L}^2(\partial\Omega)$, and $A = \Delta_\Omega$ is the Laplacian, $B = \Delta_{\partial\Omega}$ is the Laplace–Beltrami operator, and $L\colon \mathrm{H}^{1/2}(\Omega) \to \mathrm{L}^2(\partial\Omega)$ is the trace operator which describes the coupling itself.

Given the form of the problem (1.10), it seems a natural idea to use operator splitting in the following way. Choosing a time step $\tau > 0$, one can solve the problem given on the boundary with the given initial condition y_0, and obtain the value of $y(\tau)$. Using this as the boundary value, the problem inside the domain can be solved and the approximation of $x(\tau)$ obtained. Then the trace of $x(\tau)$ on the boundary becomes the initial condition of the equation for y in the next step. Iterating the above algorithm in n steps, yields the approximation of $x(n\tau)$ and $y(n\tau)$.

The "naive" algorithm presented above, however, leads to a numerical method that suffers from order reduction, i.e., does not converge with the expected order, see e.g. [86]. In [35, 36], the authors' goal was to use operator splitting to write a numerical method that converges with the expected order (first-order for Lie splitting, second-order for Strang). To do this, one needs to add an additional step to the above algorithm, namely to extend the approximation of the function $By(n\tau)$ (harmonically in case of the Laplacian) to the interior of the domain. The idea was inspired by the results of the work of [23], in which the boundary coupled problem (1.10) for $\mathcal{F} = 0$ is rewritten as an abstract initial value problem on the Banach space $\mathcal{U} := X \times Y$ for the unknown function $u = (x, y)\colon [0,\infty) \to \mathcal{U}$ of the form

$$\begin{cases} \frac{\mathrm{d}}{\mathrm{d}t}u(t) = \mathcal{A}u, & t > 0, \\ u(s) = u_0, \end{cases} \tag{1.11}$$

with

$$\mathcal{A} := \begin{pmatrix} A & 0 \\ 0 & B \end{pmatrix}, \quad D(\mathcal{A}) := \big\{(x,y) \in D(A) \times D(B)\colon Lx = y\big\}.$$

Under Assumptions 1.2.1, the result [23, Thm. 2.7] implies that $\mathcal{A}$ generates the following operator semigroup on $\mathcal{U}$:

$$\mathrm{e}^{t\mathcal{A}} = \begin{pmatrix} \mathrm{e}^{tA_0} & Q(t) \\ 0 & \mathrm{e}^{tB} \end{pmatrix}.$$

Note that if B generates an analytic semigroup, then $\mathrm{e}^{t\mathcal{A}}$ is analytic as well. With the notations

$$\mathcal{A}_0 := \begin{pmatrix} A_0 & -D_0B \\ 0 & B \end{pmatrix}, \quad D(\mathcal{A}_0) := D(A_0) \times D(B), \quad \mathcal{R}_0 := \begin{pmatrix} \mathrm{I} & -D_0 \\ 0 & \mathrm{I} \end{pmatrix}$$

one has $\mathcal{A}_0 = \mathcal{R}_0\mathcal{A}_0\mathcal{R}_0^{-1}$. To apply an operator splitting procedure, the authors write this operator as the sum $\mathcal{A}_0 = \mathcal{A}_1 + \mathcal{A}_2 + \mathcal{A}_3$, where the sub-operators and the corresponding

semigroups have the following forms on $X \times D(B)$:

$$\mathcal{A}_1 = \begin{pmatrix} A_0 & 0 \\ 0 & 0 \end{pmatrix}, \quad \mathcal{A}_2 = \begin{pmatrix} 0 & -D_0 B \\ 0 & 0 \end{pmatrix}, \quad \mathcal{A}_3 = \begin{pmatrix} 0 & 0 \\ 0 & B \end{pmatrix},$$

$$D(\mathcal{A}_1) = D(A_0) \times Y, \quad D(\mathcal{A}_2) = D(\mathcal{A}_3) = X \times D(B),$$

$$\mathrm{e}^{t\mathcal{A}_1} = \begin{pmatrix} \mathrm{e}^{tA_0} & 0 \\ 0 & \mathrm{I} \end{pmatrix}, \quad \mathrm{e}^{t\mathcal{A}_2} = \begin{pmatrix} \mathrm{I} & -tD_0 B \\ 0 & \mathrm{I} \end{pmatrix}, \quad \mathrm{e}^{t\mathcal{A}_3} = \begin{pmatrix} \mathrm{I} & 0 \\ 0 & \mathrm{e}^{tB} \end{pmatrix}.$$

In what follows the results for the linear case $\mathcal{F} = 0$ and the semilinear case $\mathcal{F} \neq 0$ will be presented.

Results in the linear case

In [35], the authors consider the linear case $\mathcal{F}_1 = \mathcal{F}_2 = 0$. Then, the solution of the boundary coupled problem (1.10) is given by $u(t) = \mathrm{e}^{t\mathcal{A}} u_0 = \mathcal{R}_0^{-1} \mathrm{e}^{t\mathcal{A}_0} \mathcal{R}_0 u_0 = \mathcal{R}_0^{-1} \mathrm{e}^{t(\mathcal{A}_1+\mathcal{A}_2+\mathcal{A}_3)} \mathcal{R}_0 u_0$. Then the operator splitting procedures are applied, and the authors obtain a numerical method of the form $u_n^{(\tau)} = \mathcal{N}(\tau)^n u_0$, where

$$\mathcal{N}(\tau) = \mathcal{R}_0^{-1} \begin{pmatrix} \mathrm{e}^{tA_0} & \mathcal{Q}(\tau) \\ 0 & \mathrm{e}^{tB} \end{pmatrix} \mathcal{R}_0, \quad \text{and}$$

$$\mathcal{Q}(\tau) = \begin{cases} -\tau \mathrm{e}^{\tau A_0} D_0 B \mathrm{e}^{\tau B} & \text{for the Lie,} \\ -\tau \mathrm{e}^{\frac{\tau}{2} A_0} D_0 B \mathrm{e}^{\frac{\tau}{2} B} & \text{for the Strang,} \\ -\frac{\tau}{2} \big(\mathrm{e}^{\tau A_0} D_0 B \mathrm{e}^{\tau B} + D_0 B \big) & \text{for the 1/2-weighted} \end{cases}$$

operator splittings, and $u_0 = (x_0, y_0)$. One can note that in all three cases the operator $\mathcal{Q}(\tau)$ is an approximation to the operator $Q_0(\tau)$.

Theorem 1.2.2 ([35, Thm. 4.9, Thm. 4.11, Thm. 4.13])**.** *For the Strang and the* 1/2*-weighted splittings, let* $\gamma \in (0, 1]$ *be a constant for which* $\operatorname{ran}(D_0) \subseteq D((-A_0)^\gamma)$ *is satisfied. Then, under Assumptions 1.2.1, for every* $T > 0$*, there exists a constant* $C > 0$*, independent of* n *and* τ*, such that the estimates of the global error of the operator splittings are satisfied:*

$$\|u(n\tau) - u_n^{(\tau)}\| \leq C\tau |\log \tau| \big(\|By_0\| + \|B^2 y_0\| \big), \quad y_0 \in D(B^2), \quad \textit{for the Lie,}$$
$$\|u(n\tau) - u_n^{(\tau)}\| \leq C\tau^{1+\gamma} |\log \tau| \big(\|By_0\| + \|B^2 y_0\| + \|B^3 y_0\| \big), \quad y_0 \in D(B^3),$$

for the Strang and the 1/2*-weighted operator splittings for all* $n = 2, 3, \ldots$ *and* $t \in [0, T]$.

In all cases, the statements follow from the result [35, Prop. 4.3], namely, that the order of the global error is the same as the order of how $\mathcal{Q}(t)$ approximates the operator $Q_0(t)$. Thus, in the proof, the authors estimate in each case the difference $\|\mathcal{Q}(\tau) - Q_0(t)\|$. To do so, they use the relation $\|(-A_0)^{1-\gamma} \mathrm{e}^{tA_0}\|_{\mathcal{L}(X)} \leq t^{\gamma-1}$ for bounded analytic semigroups and their generator, the (time) exponential boundedness of the semigroups, and the norm estimate of the local errors.

The results are also illustrated by numerical experiments. For the first problem, the exact solution is known, so the error of the numerical method can be exactly calculated. In the second case, the exact solution is not known, so the error is approximated using a reference solution. The relative global error analysed in both cases is given by

$$\varepsilon(\overline{n}_t \tau) := \frac{\|u(\overline{n}_t \tau) - u^{(\tau)}_{\overline{n}_t, \overline{n}_x}\|_2}{\|u(\overline{n}_t \tau)\|_2}$$

where $\|\cdot\|_2$ is the Euclidean norm and $u_{\overline{n}_t,\overline{n}_x} \in \mathbb{R}^{\overline{n}_x}$ is the vector of approximations of the values $(u(\overline{n}_t\tau))(jh)$, $j = 0,\dots,\overline{n}_x$, where $h > 0$ is the spatial grid size. Due to the relation $\varepsilon(\tau) \le C\tau^p$, the value of the function $\tau \mapsto \varepsilon(\tau)$ can be plotted on a logarithmic scale for certain τ values, and then by fitting a line to the resulting points, its slope gives a numerical approximation to the order of the method. This is called the numerical order of the method. Tables 1.1 and 1.2 contain the values of the numerical order. Note that in the case of $\Theta \neq \frac{1}{2}$, the authors did not analytically study the Θ-weighted splitting, but the numerical results are in line with expectations.

Table 1.1: Numerical orders of operator splittings in case of known exact solution ($\gamma = 0.25$, $\overline{n}_x = 32768$), [35, Table 1].

splitting	Lie	Strang	Weighted $\Theta = 0.3$	Weighted $\Theta = 0.5$
expected order	~ 1	~ 1.25	~ 1	~ 1.25
numerical order	1.0004	1.2405	1.0549	1.1646

Table 1.2: Numerical orders of operator splittings in case of unknown exact solution ($\gamma = 0.25$, $\overline{n}_x = 128$), [35, Table 2].

splitting	Lie	Strang	Weighted $\Theta = 0.3$	Weighted $\Theta = 0.5$
expected order	~ 1	~ 1.25	~ 1	~ 1.25
numerical order	1.0100	1.3056 for $\log\tau > -2.5$ 1.9812 for $\log\tau < -2.5$	1.0256	1.5765

The tables show that the numerical values are in agreement with the theoretical results, which can be considered as sharp in this sense. The methods developed therefore indeed converge in the expected order.

Results in the semilinear case

In [36], the authors study the semilinear case. If $\mathcal{F}_1 \neq 0$ and/or $\mathcal{F}_2 \neq 0$ in the boundary coupled problem (1.10), the solution is given by the variation of constants formula as

$$u(t) = \mathrm{e}^{t\mathcal{A}}u_0 + \int_0^t \mathrm{e}^{(t-s)\mathcal{A}}\mathcal{F}\big(u(s)\big)\,\mathrm{d}s, \quad t \ge 0,$$

where the semigroup $\mathrm{e}^{t\mathcal{A}}$ is approximated as described in the previous section:

$$\mathrm{e}^{t\mathcal{A}} \approx E_k = \begin{pmatrix} \mathrm{e}^{tA_0} & D_0\mathrm{e}^{tB} - \mathrm{e}^{tA_0}D_0 + \mathcal{Q}_k(\tau) \\ 0 & \mathrm{e}^{tB} \end{pmatrix}, \quad k = 1,2, \quad \text{where} \tag{1.12}$$

$$\mathcal{Q}_1(t) = -t\mathrm{e}^{tA_0}D_0B\mathrm{e}^{tB} \quad \text{for the Lie splitting,}$$

$$\mathcal{Q}_2(t) = -t\mathrm{e}^{\frac{t}{2}A_0}D_0B\mathrm{e}^{\frac{t}{2}B} \quad \text{for the Strang splitting.}$$

In the semilinear case, however, it is also necessary to approximate the integral, which will be done using the (first-order) left quadrature for the Lie splitting and the (second-order) midpoint quadrature for the Strang splitting. These steps will lead to a method of the form $u_n^{(\tau)} = \mathcal{N}(\tau)^n(u_0)$, $n \in \mathbb{N}$, where $\mathcal{N}(\tau)$ is now not necessarily a linear mapping:

$$\mathcal{N}(v) = \begin{cases} E_1(\tau)\big(v + \tau\mathcal{F}(v)\big) & \text{for the Lie splitting,} \\ E_2(\tau)v + \frac{\tau}{2}E_2(\tau/2)\Big(E_1(\tau/2)\big(v + \frac{\tau}{2}\mathcal{F}(v)\big)\Big) & \text{for the Strang splitting.} \end{cases}$$

The term $E_1(\tau/2)(v + \frac{\tau}{2}\mathcal{F}(v))$ in the Strang splitting formula is an approximation of the value of the function $\mathrm{e}^{(\tau-s)\mathcal{A}}\mathcal{F}(u(s))$ at $s = \tau/2$ by the Lie formula with time step $\tau/2$. The following results are obtained.

Theorem 1.2.3 ([36, Thm. 2.5]). *Under Assumptions 1.2.1, for the Lie splitting, there exist constants $\tau_0 > 0$ and $C > 0$ such that for any step size $\tau \le \tau_0$, the following error estimate holds for any $n\tau \in [0, T]$:*

$$\|u(n\tau) - u_n^{(\tau)}\| \le C\tau|\log\tau|.$$

Also in the semilinear case, the numerical results illustrate the theoretical results obtained. The numerical convergence order corresponds to the expected first order.

Relevance to dynamical networks

The above methods can be applied to dynamics on networks by writing them as boundary coupled systems (1.10). The following example illustrates how diffusion on a network with mass storage at the nodes can be expressed in the form (1.10).

Let v_i $(i = 1, \dots, n)$ and e_j $(j = 1, \dots, m)$ denote the vertices and edges of a graph, respectively. Then one chooses the spaces above as follows. The "spatial" domain is $[0, 1]$, then $X = \mathrm{L}^2(0, 1)^n$ and $Y = \mathbb{C}^m$ are the function spaces along the edges and vertices, respectively. The corresponding operators have then the forms $A = \mathrm{diag}(\partial_{xx})$ for the diffusion process inside the domain with $D(A) = \mathrm{H}^2(0, 1)^n \cap D(L)$ and $D(L) = \{x \in \mathrm{C}(0, 1)^n \colon x_j(v_i) = x_\ell(v_i)$ if $v_i = e_j \cap e_\ell\}$. Note that, by Assumption 1.2.1(iv), the restriction of operator A should generate an analytic semigroup which means that the corresponding PDE should be parabolic, hence, the diffusion process is a suitable choice. Furthermore, $B \in \mathbb{C}^{m\times m}$ then corresponds to a system of ordinary differential equations on the edges. It is worth mentioning that $\mathcal{F}_2(x, y) = Cx$ in this case, where the linear operator $(C, D(A))$ incorporates the Kirchhoff-type boundary condition posed at the vertices. Since it is unbounded, the results need to be generalized in this case.

Numerical experiments show that the results above offer reliable numerical methods which solve the dynamical network problem efficiently and converge of the expected order, that is, they do not suffer from order reduction.

1.3 Mixed Finite Elements for Euler Equations on Networks

Several models describing gas flows in pipe networks exist in the literature, see [20, 41]. Many of these are concerned with long time and space scales, which correspond to the low Mach and large friction asymptotics of the isothermal Euler equations. It is well known that classical schemes for hyperbolic conservation laws (in simple domains as well as on networks) do not work well in the low Mach regime [38], which creates a need for specific "asymptotic preserving" schemes.

In [50] the authors propose an asymptotic preserving scheme for the barotropic Euler equations, which model gas flow through (networks of) pipes. The 1-dimensional barotropic Euler equations with quadratic friction are given by

$$\begin{cases} \partial_t \rho + \partial_x m = 0, & x \in [0, \ell],\ t > 0 \\ \partial_t m + \partial_x \left(\frac{m^2}{\rho} + p(\rho) \right) = -\frac{\gamma}{\rho}|m|m, & x \in [0, \ell],\ t > 0 \end{cases} \tag{1.13}$$

on a pipe of length ℓ, where ρ is the density, $m = \rho v$ the mass flow rate, v the velocity, $p = p(\rho)$ a strictly monotone pressure law and $\gamma > 0$ a friction coefficient which describes the friction of the gas at the pipe walls. Rewriting the system in a port-Hamiltonian form and rescaling the system to long temporal and spatial scales, large friction and small, subsonic velocities, yields the system

$$\begin{cases} \partial_t \rho + \partial_x(\rho v) = 0, & x \in [0,\ell],\ t > 0 \\ \varepsilon^2 \partial_t v + \partial_x \left(\frac{1}{2}\varepsilon^2 v^2 + P'(\rho)\right) = -\gamma |v| v, & x \in [0,\ell],\ t > 0 \end{cases} \tag{1.14}$$

with scaling parameter $\varepsilon > 0$ and smooth and strictly convex pressure potential $P = P(\rho)$, which is connected to the pressure law by $p'(\rho) = \rho P''(\rho)$. Based on this system the authors define a numerical scheme by applying a mixed finite element method in space and an implicit Euler method in time. Similar schemes exist in the literature for linear wave equations [62, 80], isentropic flow in networks [47, 48], and port-Hamiltonian systems [21, 96].

The main result of [50] is the uniform convergence of the numerical scheme. More precisely, if (1.14) together with suitable boundary and initial conditions admit a subsonic, bounded state solution, then there exist $\Delta t > 0$ sufficiently small and $\Delta x \approx \Delta t$ such that the discrete scheme admits a unique discrete bounded state solution $(\rho_h^n, m_h^n)_{n \geq 0}$ which satisfies

$$\begin{aligned} &\|\rho(t^n) - \rho_h^n\|^2_{L^2(0,\ell)} + \varepsilon^2 \|m(t^n) - m_h^n\|^2_{L^2(0,\ell)} + \Delta t \sum_{i=1}^{n} \|m(t^i) - m_h^i\|^3_{L^3(0,\ell)} \\ &\leq C(\Delta t^2 + \Delta x^2), \end{aligned}$$

where the constant C can be chosen independent of ε. The proof is based on estimating the difference between the exact solution and the discrete solution in terms of relative energy, in similar fashion to [49].

The scheme and convergence result can be extended to networks by complementing the system with coupling conditions enforcing conservation of mass and continuity of the specific enthalpy $h := \frac{1}{2}\varepsilon^2 v^2 + P(\rho)$. These are energy conserving at pipe junctions [117], hence one may exploit the Hamiltonian formulation to arrive at the extension.

1.4 Numerical Approximation and Control of PDEs on Networks via Random Batch Methods

The Random Batch Method (RBM) is a numerically efficient technique for solving large scale dynamical systems, originally introduced in the context of interacting particle systems [22, 78, 79]. This method efficiently combines the random nature of stochastic gradient descent with the strategy of dividing data into smaller groups or batches. It is therefore inspired by classical domain decomposition and splitting techniques, but with the added feature of randomization, which reduces the computational cost, given that large dimensional systems can be intractable in the deterministic setting.

Investigating the RBM in control for both finite-dimensional and systems of partial differential equations (PDEs), with an aim to provide rigorous proofs of convergence and combine it with Model Predictive Control (MPC), is the focus of one of the members of the Action, in conjunction with others in their group. The main results in these directions are as follows:

In [134], considering linear finite dimensional systems and using matrix decomposition it is shown that the solution of such a randomized dynamical system closely approximates that of the original system in expectation, provided that the time steps are sufficiently small.

In addition, the linear quadratic regulator control problem was analyzed and similar convergence results were achieved. These results were extended in the context of Model Predictive Control (MPC), [84, 133].

In the forthcoming paper [75], the authors extend this analysis to PDEs in networks, using the combination of the numerical approximation of the PDE by classical finite-difference and finite-element schemes and the RBM-MPC methodology above. This allows to exploit the splitting of the network into subnetworks, implemented, for instance, by spectral techniques, along the nodal sets of the eigenfunctions of the Laplacian or the governing operator (see Figure 1.1).

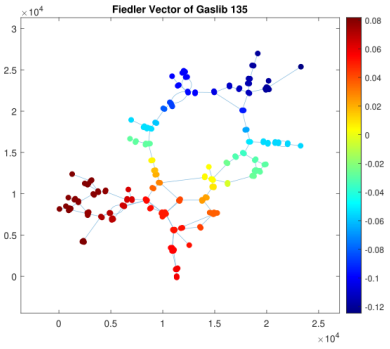

Figure 1.1: A complex graph decomposed into subgraphs, represented by various colours, by means of spectral clustering. This decomposition offers a natural splitting method to apply the combination of RBM-MPC. It also induces a natural partitioning of the matrices involved in the discretized dynamics.

1.5 A Physics Informed Neural Network Preserving Energy Dissipation of Allen-Cahn Equations

With advances in computing power and the rapid growth of available data in recent years, deep learning techniques, a subset of machine learning, have become a promising and popular methodology to solve different types of problems in science and engineering. Deep learning is principally based on complex, non-linear combinations of input and output features using multiple hidden layers and the back-propagation algorithm, which works by increasing the weights of the combinations which are judged to be "useful" (i.e. which produce good results) during the training process, and decreasing the weights of others.

Alongside the remarkable success of deep learning in such various fields as visual recognition [89] and cognitive science [92], efforts have also been made to use deep learning to solve partial differential equations (PDEs); see, e.g, [46, 95, 115, 125]. Among them, Physics Informed Neural Networks (PINNs), introduced in [115], have received great attention thanks to their flexibility in tackling a wide range of forward and inverse problems involving PDEs. To predict the dynamics of the underlying PDE, the physics of the problem is imposed on the loss function in the PINN architecture by adding governing equations, boundary conditions, and initial conditions. Since their introduction, PINNs have been used to solve a variety of problems in computational science and engineering; see, e.g., [25, 82, 101, 103] and references therein.

Although the standard PINN (std-PINN) has been widely accepted and has yielded remarkable results across a range of problems, it is not always capable of solving nonlinear PDEs

containing sharp transition layers, discontinuities, or shocks, such as the Allen–Cahn equation [2]. To improve the performance of PINNs while solving Allen–Cahn equations, the authors in [61] proposed two specially designed convolutional neural networks (CNNs) in which the loss functions correspond to the fully-discrete systems obtained from finite difference methods in both space and time. Similarly, multi-step discrete time models with adaptive collocation strategy were considered in [137]. The authors in [136] introduced the idea of adaptivity in both time and space by sampling the data points, while in [104], the same neural network was retrained over successive time segments, while satisfying the obtained solution for all previous time segments. An alternative approach considered by [124] consists of reducing the system of the Allen–Cahn equation to first-order problem and subsequently using deep learning to approximate the converted minimization problem.

The authors of [91] propose a novel methodology based on preserving the energy dissipation to predict the dynamics of the Allen-Cahn equation. The proposed network approach, outlined below, guarantees the decay of energy and also plays a key role in accurately learning the dynamics of the Allen-Cahn equation.

Allen–Cahn equations

Allen–Cahn equations were introduced in [2] to describe the motion of anti-phase boundaries in crystalline solids at a fixed temperature. They are a particular case of gradient flows in the form of

$$\partial_t u = -\mu(u)\ \frac{\delta \mathcal{E}(u)}{\delta u},$$

where $\delta\mathcal{E}(u)/\delta u$ represents the variational derivative of the free energy taken in the $\mathrm{L}^2(\Omega)$-norm with $\Omega \subset \mathbb{R}^d$ $(d = 1, 2, 3)$ as follows

$$\mathcal{E}(u) = \int_\Omega \left(\frac{\epsilon^2}{2} |\nabla u|^2 + F(u) \right) \mathrm{d}x.$$

Then, the Allen–Cahn equation is given by

$$\partial_t u = \mu(u)(\epsilon^2 \Delta u - f(u)), \quad (x, t) \in \Omega \times (0, T], \tag{1.15}$$

where u denotes the concentration of one of the species of the alloy, ϵ represents the small interfacial length during the phase separation process, and $\mu(u)$ is the non–negative mobility function. The nonlinear function $f(u)$ is the derivative of a quartic double–well free energy functional $F(u) = \frac{1}{4}(1-u^2)^2$. Further, the total free energy of Allen–Cahn equations decreases with time for $\mu(u) > 0$, that is,

$$\frac{\mathrm{d}\mathcal{E}(u(t))}{\mathrm{d}t} \leq 0. \tag{1.16}$$

However, it is not always easy to satisfy the energy dissipation (1.16) numerically due to the existence of a nonlinear term and of the small interfacial length parameter ϵ. Motivated by the conservation of the related quantities, such as mass, energy, and momentum, the authors of [91] propose the penalization of the energy constraint (1.16) in order to preserve the energy decay of the Allen–Cahn equations (1.15).

Numerical algorithm and results

The PINN architecture used to investigate the dynamics of a one-dimensional Allen–Cahn equation with periodic boundary conditions is depicted in Figure 1.5. Figure 1.3 indicates that the learned solutions are accurate and capture the correct dynamics when compared with the reference solution, obtained by using the `chebfun` package [44]. In Table 1.3, the performance of the new approach (named "Energy-PINN") is compared with different existing approaches in the literature; see, e.g., [104, 115, 136]. Note that strategies based on adaptive approaches to classical numerical techniques are also used in the numerical simulations. It is observed that the Energy-PINN method is highly accurate in comparison to other methods.

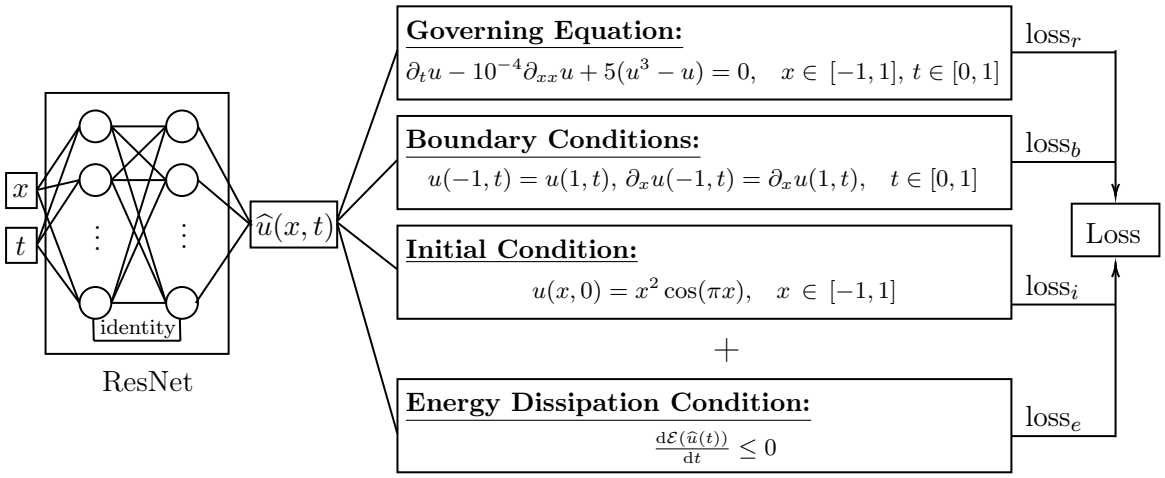

Figure 1.2: Workflow of the proposed PINN framework.

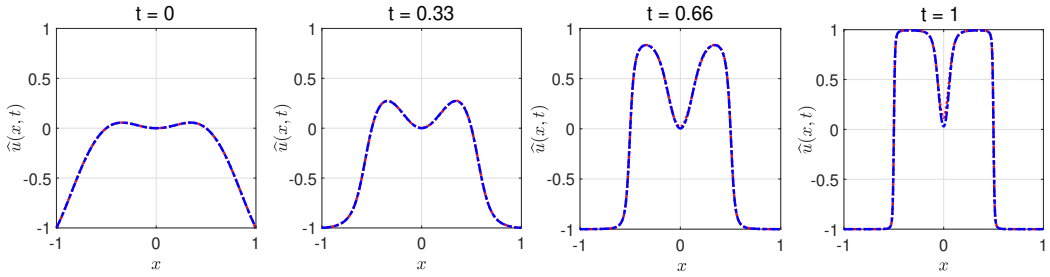

Figure 1.3: Predicted (red) and reference (blue) solutions.

Table 1.3: Performance comparison.

Method	**relative ℓ_2-norm**
std-PINN [115]	0.9919
XPINN [77]	0.9612
bc-PINN [104]	0.0701
bc-PINN + logresidual [104]	0.0300
ACP [136]	0.0233
bc-PINN + ICGL + TL [104]	0.0168
Energy-PINN	0.0053

1.6 Homogenization Problems on Graphs

This section addresses two instances of homogenization problems posed on periodic planar graphs.

In the first problem one considers time-dependent heat conduction on a planar one-dimensional periodic network structure with periodic unit cell Γ_Y. This simple problem provides a useful setting in which to develop techniques necessary for the homogenization of equations posed on graphs, see [99]. On the edges of a graph the one-dimensional heat equation is posed, while the Kirchhoff junction condition is applied at all (inner) vertices. Using the two-scale convergence adapted to homogenization of lower-dimensional problems one can obtain the limit homogenized problem defined on a two-dimensional domain that is occupied by the mesh when the mesh period δ tends to 0. The homogenized model is given by the classical heat equation with the conductivity tensor depending on the unit cell graph only through the topology of the graph and lengths of its edges. In [99] it is proven that the sequence of solutions of heat conduction problems on a graph (two-scale) converges to the function u^0 which is the unique solution of the following problem:

$$\text{Find} \quad u^0 \in \mathrm{L}^2(0,T;\mathcal{H}) \quad \text{such that} \quad \partial_t u^0 \in \mathrm{L}^2(0,T;\mathrm{L}^2(\Omega)),$$

where $\mathcal{H} = \{v \in \mathrm{H}^1(\Omega) : v = 0 \text{ on } \Gamma_D\}$, such that for all $v \in \mathcal{H}$

$$\int_\Omega \rho c_p \partial_t u^0(t,\mathbf{x}) v(\mathbf{x}) \mathrm{d}\mathbf{x} + \int_\Omega a(\mathbf{x}) \mathbf{A}^{\mathrm{hom}} \nabla u^0(t,\mathbf{x}) \cdot \nabla v(\mathbf{x}) \mathrm{d}\mathbf{x} = \int_\Omega f_{\mathrm{hom}}(t,\mathbf{x}) v(\mathbf{x}) \mathrm{d}\mathbf{x}, \tag{1.17a}$$

$$u^0(0,\mathbf{x}) = u_{\mathrm{init}}(\mathbf{x}), \qquad \mathbf{x} \in \Omega, \tag{1.17b}$$

where u_{init} is the initial condition, the homogenized source is given by

$$f_{\mathrm{hom}} := \frac{1}{|\Gamma_Y|} \int_{\Gamma_Y} f(\cdot,\cdot,\mathbf{y}) \, \mathrm{d}s(\mathbf{y}) \tag{1.18}$$

and where the constant 2-by-2 symmetric and positive definite matrix $\mathbf{A}^{\mathrm{hom}}$ (homogenized tensor) is given by

$$\mathbf{A}^{\mathrm{hom}} := \frac{1}{|\Gamma_Y|} \int_{\Gamma_Y} (\mathbf{t}(\mathbf{y}) + \partial_\Gamma \phi(\mathbf{y})) (\mathbf{t}(\mathbf{y}) + \partial_\Gamma \phi(\mathbf{y}))^T \, \mathrm{d}s(\mathbf{y}), \tag{1.19}$$

where $\phi \in \mathrm{H}^1_\#(\Gamma_Y)^2$, i.e. the space of periodic H^1 functions, is the unique solution (up to an additive constant) of the canonical problem on the unit cell Γ_Y

$$\int_{\Gamma_Y} \partial_\Gamma \phi(\mathbf{y}) \partial_\Gamma \psi(\mathbf{y}) \, \mathrm{d}s(\mathbf{y}) = -\int_{\Gamma_Y} \mathbf{t}(\mathbf{y}) \partial_\Gamma \psi(\mathbf{y}) \, \mathrm{d}s(\mathbf{y}), \qquad \forall \psi \in \mathrm{H}^1_\#(\Gamma_Y). \tag{1.20}$$

Here $\mathbf{t}$ is the unit tangent line on the graph edge and ∂_Γ denotes the tangential derivative on edges. In [99] the well-posedness of the limit problem is shown and a purely algebraic formula for the computation of the homogenized conductivity tensor is given. The analysis is complemented by numerical experiments showing a convergence to the limit problem where the convergence order depends on the unit cell pattern Γ_Y.

The second problem considers the homogenization of the equilibrium of a periodic plane network of elastic rods with the unit cell Γ_Y. In this case the standard reference is [28] where a simple plus sign unit cell geometry is analyzed by first taking the thickness of the

plate to zero, then performing homogenization of the obtained plate type equation and then taking the horizontal thickness of bars to zero. Alternatively, [53] and [26] consider the same problem, but the authors begin by homogenizing and then take first the plate thickness and second the horizontal thickness to zero. Another approach can be found in [65] and [27] where simultaneous homogenization and dimension reduction is made. The obtained cell problem, typical in homogenization is then a 3D problem.

In contrast to the above mentioned approaches the authors of [98] model elastic rods by a Naghdi/Timoshenko type one-dimensional curved rod model and replace the 3D model by the 1D model and then homogenize, treating rod thickness as a small parameter of the cell size. Using techniques developed in [99] one can derive the model for the structure under the transversal forcing. The novelty of the approach in [98] is twofold. Firstly, homogenization is performed on a system of ordinary differential equations on a graph. Secondly, while this type of problem has been analyzed for general scalar second or fourth order problems in [144], [15] and [17], it is newly applied to the 1D model of elastic rods. Related to the elasticity problem of thin rod-like structures, the measure fattening approach has been applied in [16] and [144] making 3D structure from the graph and using the two-scale convergence with respect to measure.

The limit model obtained in [98] is given by a fourth order equation in the form of an elastic plate equation formulated on a two-dimensional domain with effective elasticity coefficients that depend on the local graph geometry in the local unit cell as is typical in homogenization. The homogenized problem for the transversal displacement u_3^0 is given by:

$$\begin{aligned} &\text{Find } u_3^0 \in \mathcal{V} = \{v \in \mathrm{H}^2(\Omega) : v|_{\partial\Omega} = 0\} \text{ such that} \\ &\int_\Omega \mathbf{A}_{\mathrm{hom}} \nabla^2 u_3^0 \cdot \nabla^2 v_3 \,\mathrm{d}\mathbf{x} = \int_\Omega f_{\mathrm{hom},3} v_3 \,\mathrm{d}\mathbf{x}, \end{aligned} \tag{1.21}$$

where $v_3 \in \mathcal{V}$ and the homogenized tensor $\mathbf{A}_{\mathrm{hom}}$ is given in terms of the solution of four canonical problems on the unit cell Γ_Y. These canonical problems are given as a system of ordinary differential equations on the unit cell Γ_Y which formulate the one-dimensional model for thin rod-like elastic structures. For the cell structures with piecewise straight edges the effective coefficients can be calculated as an exact solution of a system of algebraic equations. Based on this result, in [98] the homogenized tensor is compared – for several unit cell geometries – with the results from [53] and [28] and different coefficients in the equation are obtained. This non-commutativity of the limits is typical in homogenization and dimension reduction.

Chapter 2

Control of PDEs on Networks

2.1 Limits of Stabilization for Networked Hyperbolic Systems

In many papers on the control of networks, the analysis is restricted to the case of tree-shaped graphs. However, it is very important to collect knowledge about the effect of cycles in the network. In [71], this is done for a networked system where the dynamics on each edge are governed by a wave equation with a linear source term. At the vertices, the states are coupled by node conditions that require the continuity of the state and that the normal derivatives sum up to zero. In order to assess the limits of controllability a specific example is studied: A network consisting of a circle and two additional edges, where both arcs of the circle have the same lengths. Feedback control occurs at one boundary node, while a Dirichlet boundary

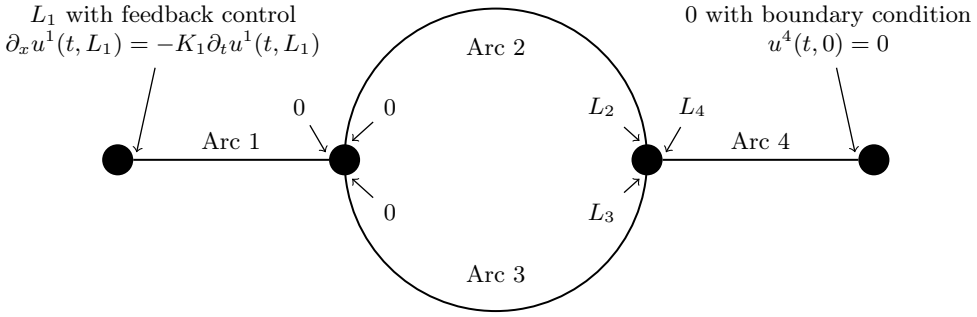

Figure 2.1: Diagram of the considered example network

condition is prescribed at the other. For $k \in \{1, 2, 3, 4\}$ let real numbers $c_k > 0$, $\varepsilon_k \geq 0$ be given, then the following system is considered where each pipe is parameterized from 0 to $L_k > 0$ where L_k is its length:

$$\begin{cases} \partial_{tt} u^k = \partial_{xx} u^k - 2\varepsilon_k \partial_t u^k - (\varepsilon_k^2 - c_k^2) u^k, \quad t \in (0, +\infty),\ x \in [0, L_k],\ k \in \{1, 2, 3, 4\}, \\ u^1(t, 0) = u^2(t, 0) = u^3(t, 0), \\ u^2(t, L_2) = u^3(t, L_3) = u^4(t, L_4), \\ \Sigma_{k=1,2,3} \partial_x u^k(t, 0) = 0, \\ \Sigma_{k=2,3,4} \partial_x u^k(t, L_k) = 0, \\ u^4(t, 0) = 0, \\ \partial_x u^1(t, L_1) = -K_1 \partial_t u^1(t, L_1). \end{cases} \tag{2.1}$$

It is shown that the system is stabilizable if the lengths of the arcs in the cycle are sufficiently small. However, if the lengths of the arcs are too large, the system is not stabilizable. It is shown that the situation is robust with respect to small perturbations of the arc lengths. This shows that the length of the edges is a decisive parameter in the study of boundary control problems for systems with a cycle.

2.2 Boundary Null Controllability of Strongly Degenerate Hyperbolic Systems on a Star-Shaped Planar Network

This section describes recent progress in the study of boundary exact null controllability for the simplified one-dimensional hyperbolic model of a multi-body structure consisting of a finite number of flexible strings distributed along a star-shaped network with a defect at the common node. In principle, damage modeling is a well-understood topic in continuum mechanics. However, when it comes to optimal control problems for degenerate hyperbolic equations posed on singular graphs, despite the practical relevance of such systems, the theory remains underdeveloped. A simple illustration of the usefulness of these problems is the following: a given serially connected system of beams (or bars) will probably develop damage at the connection point if that point is a result of welding or gluing.

In the one-link case, which considers e.g. a single string or beam, damage is only modeled at the ends. In contrast, for a serial or more general network structure as considered below, the transmission conditions at nodes where damage occurs depend on the kind of traces that can be drawn from functions and their derivatives at such nodes, and as such can be difficult to determine. This makes constructing the network out of single elements using anticipated transmission conditions at the nodes extremely challenging.

As a result, the authors of [85] instead use singular measures as support for a given string in the network in order to model planar networks of scalar strings. They consider the present activity in this field as the first attempt to investigate this class of problems from a mathematical control perspective in the context of partial differential equations on metric graphs.

Statement of the problem

Let Ω be an open bounded set in $\mathbb{R}^2$ such that 0 is an interior point and Ω has a sufficiently smooth boundary $\partial\Omega$. Let $I_1, I_2, \dots, I_N$ be a collection of segments starting at the origin and directed along the vectors $v_1, v_2, \dots, v_N$. The remainder of the discussion rests on the following assumptions:

Assumptions 2.2.1. *1.* $\frac{v_i}{|v_i|} \neq \frac{v_j}{|v_j|}$ *for* $i \neq j$,

2. $I_i \subset \Omega \; \forall\, i = 1, \dots, N$, *and*

3. all the end points of these segments $K = \{M_i,\ i = 1, \dots, N\}$ *belong to the boundary,* $K \subset \partial\Omega$.

The length of the segment I_i is denoted by ℓ_i. In the sequel, the object $G = \big(K \cup \{0\}, \{I_1, \dots, I_N\}\big)$ is called a *star-shaped planar network*. On each interval (edge of the network) one chooses an orientation in accordance to the direction of the vectors v_i. As a result, I_i can be parametrized as a function of its length by means of the function $z_i : [0, \ell_i] \to I_i$, i.e.,

$$z_i(\xi) = \xi \frac{v_i}{|v_i|_{\mathbb{R}^2}},\ \forall\, \xi \in [0, \ell_i],\ |z_i(\xi)| = \sqrt{z_{i,1}^2 + z_{i,2}^2} = \xi,\ \text{and}\ z_i(\ell_i) = M_i.$$

Definition 2.2.2. *A function* $a \colon \Omega \to \mathbb{R}$ *is called an* admissible weight function *if:*

(i) $a \in C(\overline{\Omega}) \cap C^1(\overline{\Omega} \setminus \{0\})$;

(ii) $a(0) = 0$ *and* $a(x) > 0$ *for each* $x \in \overline{\Omega} \setminus \{0\}$;

(iii) There exists an open convex neighbourhood $\mathcal{U} \subset \Omega$ of the origin in $\mathbb{R}^2$ such that

$$\begin{aligned} &(\nabla a(x), x)_{\mathbb{R}^2} > 0 \quad \forall\, x \in (I_i \cap \mathcal{U}) \setminus \{0\}, \\ &\eta_{i,a} := \sup_{x \in I_i \cap \mathcal{U}} \frac{(\nabla a(x), x)_{\mathbb{R}^2}}{a(x)} = \lim_{x \to 0, x \in I_i \cap \mathcal{U}} \frac{(\nabla a(x), x)_{\mathbb{R}^2}}{a(x)} < 2, \\ &a\left(\left[\frac{v_i}{|v_i|}\right]\right) \in C^{[\eta_{i,a}]}\left([0, \ell_i]\right) \end{aligned} \tag{2.2}$$

for each $i \in \{1, \dots, N\}$, where $[\cdot]$ stands for the integer part.

The points where the intervals I_i intersect the boundary of the neighbourhood $\mathcal{U}$ are denoted L_i for each $i = 1, \dots, N$. So, $I_i \cap \partial\mathcal{U} = \{L_i\}$ and so $L_i = \ell_i^* \frac{v_i}{|v_i|}$ for some $\ell_i^* \in (0, \ell_i]$. Moreover, if $a : \Omega \to \mathbb{R}$ is an admissible weight function, then relation (2.2) implies that, for each $i \in \{1, \dots, N\}$, the mapping $x \mapsto a(x)$ is monotonically increasing along the interval $(I_i \cap \mathcal{U}) \setminus \{0\}$.

With each segment I_i, one associates a singular measure μ_i concentrated on it, where it is assumed that μ_i is uniformly distributed on I_i and coincides with Lebesgue measure $\mathcal{L}^1$. Setting $\mathrm{d}\mu = \sum_{i=1}^N \mathrm{d}\mu_i$, one can see that μ is a singular measure with respect to the Lebesgue measure $\mathcal{L}^2$, and $\mu\left(\Omega \setminus \cup_{i=1}^N I_i\right) = 0$. Therefore, any functions $f = f(x)$ and $g = g(x)$ taking the same values on the planar network G coincide as elements of $L^1(\Omega, \mathrm{d}\mu)$, provided they have finite norms in this Lebesgue space.

In [85] the authors study the well-posedness and boundary controllability of the following Cauchy–Dirichlet problem

$$\begin{cases} \partial_{tt} u - \operatorname{div}^\mu(a \nabla^\mu u) = 0 & \text{in } (0, \infty) \times \Omega, \\ u(t, M_i) = f_i(t) & \text{for a.a. } t \in (0, \infty) \text{ and } i = 1, \dots, N, \\ u(0, x) = y_0(x), \quad u_t(0, x) = y_1(x) & \text{for } \mu\text{-a.a. } x \in \Omega, \end{cases} \tag{2.3}$$

where (y_0, y_1) is a given initial state, $a : \Omega \to \mathbb{R}$ is a weight function with properties (i)–(iii), and $f_i \in \mathrm{L}^2_{\mathrm{loc}}(0, \infty)$, $i = 1, \dots, N$, are control functions. Here, $\nabla^\mu u$ stands for some μ-gradient of the function u, and div^μ is the divergence operator with respect to the singular measure μ.

The degeneracy of the hyperbolic system (2.3) at the central node $x = 0$ is proposed to be measured by the parameter η_a which is defined as

$$\eta_a = \max_{i \in \{1, \dots, N\}} \left[\lim_{\xi \to 0+} \frac{\xi}{a\left(\xi \frac{v_i}{|v_i|}\right)} \frac{\mathrm{d}}{\mathrm{d}\xi} a\left(\xi \frac{v_i}{|v_i|}\right) \right],$$

where $\frac{(\nabla a(x), v_i)_{\mathbb{R}^2}}{|v_i|_{\mathbb{R}^2}} = \frac{\mathrm{d}a}{\mathrm{d}v_i}$ is the directional derivative of $a = a(x)$ along the vector v_i. In particular, (2.3) is *weakly degenerate* if $\eta_a \in [0, 1)$ and *strongly degenerate* if $\eta_a \in [1, 2)$. It is shown in [85] that the boundary observability and null controllability properties no longer hold true if $\eta_a \geq 2$. In particular, the observability time blows up when η_a converges to 2 from below.

The main result of [85] can be stated as follows:

Theorem 2.2.3. *Let $a \colon \overline{\Omega} \to \mathbb{R}$ be a weight function satisfying properties (i)–(iii) in Definition 2.2.2 and*

$$\frac{\mathrm{d} \ln a\left(\xi \frac{v_i}{|v_i|}\right)}{\mathrm{d}\xi} \leq \frac{\mathrm{d} \ln \xi^{\eta_{i,a}}}{\mathrm{d}\xi}, \quad \forall\, \xi \in [\ell_i^*, \ell_i], \quad \forall\, i = 1, \dots, N.$$

Let T_a be a value defined as

$$T_a = \frac{4\sum_{i=1}^{N} \max\left\{1, \frac{(\ell_i^*)^2}{a(L_i)}, \frac{(\ell_i)^2}{\min\limits_{x\in[L_i,M_i]} a(x)}\right\}}{2-\max\{\eta_{1,a},\dots,\eta_{N,a}\}} + \frac{2\max\{\eta_{1,a},\dots,\eta_{N,a}\}\sum_{i=1}^{N} C_{i,a}}{2-\max\{\eta_{1,a},\dots,\eta_{N,a}\}},$$

Then, for any $T > T_a$ and $(y_0, y_1) \in \mathrm{L}^2(\Omega, \mathrm{d}\mu) \times W_a^{-1,2}(\Omega, \mathrm{d}\mu)$, there exists a control function $F = [f_1, f_2, \dots, f_N]^t \in \mathrm{L}^2(0, T; \mathbb{R}^N)$ such that the corresponding solution of (2.3) (in the sense of transposition) satisfies condition $(y(T), y_t(T)) \equiv (0, 0)$, i.e. the system (2.3) is boundary null controllable in time $T > T_a$.

2.3 Controllability of Linear Advection-Diffusion Equations on Networks and Vanishing Viscosity Limit

In the preprint [11], the authors study a linear advection-diffusion equation on a tree-shaped network:

$$\begin{cases} a^e \partial_t y_\varepsilon^e(t,x) + b^e \partial_x y_\varepsilon^e(t,x) - \varepsilon \partial_{xx} y_\varepsilon^e(t,x) = 0, & t \in (0,T),\ x \in e,\ \forall e \in \mathcal{E}, \\ y_\varepsilon^e(t,v) = u_\varepsilon^v(t), & t \in (0,T),\ v \in \mathcal{V}_\partial, \\ y_\varepsilon^{e_1}(t,v) = y_\varepsilon^{e_2}(t,v), & t \in (0,T),\ v \in \mathcal{V}_0,\ \forall e_1, e_2 \in \mathcal{E}(v), \\ \sum_{e\in\mathcal{E}(v)} b^e y_\varepsilon^e(t,v) n^e(v) - \varepsilon \partial_{n^e(v)} y_\varepsilon^e(t,v) = 0, & t \in (0,T),\ v \in \mathcal{V}_0, \\ y_\varepsilon^e(0,x) = y_0^e(x), & x \in e,\ \forall e \in \mathcal{E}, \end{cases} \tag{2.4}$$

where $a^e, b^e, \varepsilon > 0$, and $T > 0$ is a fixed time-horizon, and $\partial_{n^e(v)} y_\varepsilon^e := n^e(v)\partial_x y_\varepsilon^e(v)$.

The well-posedness of this model was studied by other members of the Action in [52]; the coupling conditions ensure the conservation of mass, energy dissipation, and continuity at the junctions. For completeness, some notation for discussing networks is detailed here:

- the network is represented by a finite, directed, and connected graph $\mathcal{G} = (\mathcal{V}, \mathcal{E})$ with vertices $\mathcal{V} = \{v_1, \dots, v_n\}$ and edges $\mathcal{E} = \{e_1, \dots, e_m\} \subset \mathcal{V} \times \mathcal{V}$,
- $\mathcal{E}(v) = \{e \in \mathcal{E} : e = (v, \cdot) \text{ or } e = (\cdot, v)\}$ is the set of edges incident to the vertex $v \in \mathcal{V}$,
- $\mathcal{V}_\partial = \{v \in \mathcal{V} : |\mathcal{E}(v)| = 1\}$ is the set of boundary vertices (here $|S|$ denotes the cardinality of a set S),
- $\mathcal{V}_0 = \mathcal{V} \backslash \mathcal{V}_\partial = \{v \in \mathcal{V} : |\mathcal{E}(v)| \geq 2\}$ is the set of internal vertices,
- for every edge $e = \left(v^{\text{in}}, v^{\text{out}}\right)$, the numbers $n_e\left(v^{\text{in}}\right) := -1$ and $n_e\left(v^{\text{out}}\right) := 1$ are used to indicate the start and end point of the edge; $n_e(v) := 0$ for $v \in \mathcal{V} \setminus \left\{v^{\text{in}}, v^{\text{out}}\right\}$,
- for every vertex $v \in \mathcal{V}$, the set $\mathcal{E}(v)$ is split into $\mathcal{E}^{\text{in}}(v) := \{e \in \mathcal{E} : n_e(v) > 0\}$ and $\mathcal{E}^{\text{out}}(v) := \{e \in \mathcal{E} : n_e(v) < 0\}$, which are the sets of edges pointing into and out of the vertex v, respectively,
- $\mathcal{V}_\partial$ is split into a set of boundary vertices, $\mathcal{V}_\partial^{\text{in}} := \{v \in \mathcal{V}_\partial : n_e(v) < 0 \text{ for } e \in \mathcal{E}(v)\}$, from which edges leave into the network, and its complement $\mathcal{V}_\partial^{\text{out}} := \{v \in \mathcal{V}_\partial : n_e(v) > 0 \text{ for } e \in \mathcal{E}(v)\}$.

The authors of [11] aim to steer the solution of (2.4) to zero by using controls localized in the boundary vertices and to study the asymptotic behavior of the "cost of null-controllability" as the viscosity parameter vanishes. While this type of controllability result on networks was previously well-understood (modifying arguments in [76]), the work focuses on keeping track of the cost of null-controllability as the diffusivity ε approaches zero, which is already challenging on a segment [34]. Indeed, no results were previously available on uniform controllability in the context of singular limits on networks, despite the problem's long history on Euclidean domains (going back to, e.g., [34]).

The first observation is that the solution of (2.4) converges to that of the hyperbolic problem

$$\begin{cases} a^e \partial_t y^e(t,x) + b^e \partial_x y^e(t,x) = 0, & t \in (0,T),\ x \in e,\ \forall e \in \mathcal{E}, \\ y^e(t,v) = u^v(t), & t \in (0,T),\ v \in \mathcal{V}_\partial^{\text{in}}, \\ y^{e_1}(t,v) = y^{e_2}(t,v), & t \in (0,T),\ v \in \mathcal{V}_0,\ \forall e_1, e_2 \in \mathcal{E}^{\text{out}}(v), \\ \sum_{e \in \mathcal{E}^{\text{in}}(v)} b^e y^e(t,v) = y^{e_1}(t,v) \sum_{e \in \mathcal{E}^{\text{out}}(v)} b^e, & t \in (0,T),\ v \in \mathcal{V}_0,\ e_1 \in \mathcal{E}^{\text{out}}(v), \\ y^e(0,x) = y_0^e(x), & x \in e,\ \forall e \in \mathcal{E}, \end{cases} \tag{2.5}$$

as $\varepsilon \to 0^+$. Additionally, as a consequence of the method of characteristics, the system (2.5) is null-controllable for sufficiently large times and not controllable for small times. Thus, the natural conjecture is that, for small times, the cost of null-controllability of (2.4) explodes as $\varepsilon \to 0^+$; whereas, for T sufficiently large, it decays to zero as $\varepsilon \to 0^+$. To prove (a quantitative version of) these claims, several technical innovations are needed.

The core strategy is based on the classical *Hilbert Uniqueness Method* (H.U.M., see [97]). In this context, to prove the blow-up, the key tools are an Agmon-type inequality and the construction of a suitable datum for the adjoint system; to prove the decay, there are two ingredients: using a decay property for the L^2-mass of the adjoint system and then a Carleman-type inequality (keeping track of the viscosity parameter). The proof of the Carleman inequality is particularly challenging and of interest due to the presence of boundary terms at the junctions: in particular, an important technical innovation is the introduction of new suitable weights of *Fursikov–Imanuvilov* type (see [59]) using a piecewise-C^2 auxiliary function.

Controllability of conservation laws on networks

In [37], the authors study the controllability of a nonlinear conservation law on a star-shaped graph:

$$\begin{cases} \partial_t u_i + \partial_x f_i(u_i) = 0, & t > 0,\ x \in (-L_i, 0), \\ \partial_t u_j + \partial_x f_j(u_j) = 0, & t > 0,\ x \in (0, L_j), \\ u_i(0,x) = u_{0,i}(x), & x \in (-L_i, 0), \\ u_j(0,x) = u_{0,j}(x), & x \in (0, L_j), \\ u_i(t,-L_i) = u_{b,i}(t), & t > 0, \\ \sum_{i=1}^n f_i(u_i(t,0-)) = \sum_{j=n+1}^{n+m} f_j(u_j(t,0+)), & t > 0, \end{cases} \tag{2.6}$$

where $L_i, L_j > 0$, $i \in \{1, \dots, n\}$, $j \in \{n+1, \dots, n+m\}$, and the flux functions satisfy suitable assumptions (including a monotonicity condition $f_\ell' \geq 0$, for $\ell \in \{1, \dots, n+m\}$). For this problem, a notion of entropy-admissible solution has already been developed (see [5, 57, 109]).

The main result of [37] generalizes an approach used by Donadello and Perrollaz in [42]. By relying on an L^1-based Lyapunov functional, it is possible to deduce a controllability-to-trajectories result for such entropy solutions (acting on the exterior boundary nodes) requiring

only geometric monotonicity-type conditions, rather than convexity/concavity assumptions on the flux, as is more classical in the literature.

Furthermore, the robustness of this result with respect to viscous perturbations is discussed.

Zero diffusion-dispersion limit for the Benjamin–Bona–Mahony–Burgers equation at a junction

In the work in progress [24], the authors consider the following *generalized Benjamin–Bona–Mahony–Burgers equation*, which contains diffusive and dispersive effects, on a star-shaped graph:

$$\begin{cases} \partial_t \rho_{i,\varepsilon,\delta} + \partial_x f(\rho_{i,\varepsilon,\delta}) = \varepsilon \partial_{xx} \rho_{i,\varepsilon,\delta} + \delta \partial_{txx} \rho_{i,\varepsilon,\delta}, & t>0,\ x<0, \\ \partial_t \rho_{j,\varepsilon,\delta} + \partial_x f(\rho_{j,\varepsilon,\delta}) = \varepsilon \partial^2_{xx} \rho_{j,\varepsilon,\delta} + \delta \partial_{txx} \rho_{j,\varepsilon,\delta}, & t>0,\ x>0, \\ \rho_{i,\varepsilon,\delta}(t,0) = \rho_{j,\varepsilon,\delta}(t,0), & t>0, \\ \sum\limits_{i=1}^{n} \left(f(\rho_{i,\varepsilon,\delta}(t,0)) - \varepsilon \partial_x \rho_{i,\varepsilon,\delta}(t,0) - \delta \partial_{tx} \rho_{i,\varepsilon,\delta}(t,0) \right) & \\ = \sum\limits_{j=n+1}^{n+m} \left(f(\rho_{j,\varepsilon,\delta}(t,0)) - \varepsilon \partial_x \rho_{j,\varepsilon,\delta}(t,0) - \delta \partial_{tx} \rho_{j,\varepsilon,\delta}(t,0) \right), & t>0, \\ \rho_{i,\varepsilon,\delta}(0,x) = \rho_{i,\varepsilon,\delta,0}(x), & x<0, \\ \rho_{j,\varepsilon,\delta}(0,x) = \rho_{j,\varepsilon,\delta,0}(x), & x>0, \end{cases} \tag{2.7}$$

where $\varepsilon,\ \delta > 0$, $i \in \{1,...,n\}$, $j \in \{n+1,...,n+m\}$, and f is a genuinely nonlinear flux function. The transmission conditions at the junction $x = 0$ in (2.7) give the continuity of traces of the solution and mass-conservation.

The well-posedness of (2.7) (under suitable assumptions on the flux function and initial data) was studied in [106].

The authors are interested in investigating the zero diffusion-dispersion limit: they prove that, as the diffusion and dispersion parameters $\varepsilon,\ \delta > 0$ go to zero (under suitable balance conditions), the solution of (2.7) converges to the entropy-admissible solution of the corresponding conservation law (in the sense of [5]).

While the vanishing viscosity limit has previously been extensively studied (see, e.g., [5, 30]), the zero diffusion-dispersion singular limit problem presents several technical challenges due to the dispersive effects (namely, lack of uniform L^∞-estimates). The key tool in the proof is the L^p compensated compactness framework introduced by Schonbek in [122]. This is the first work on diffusive-dispersive singular limits on networks.

Chapter 3

Numerically Efficient H_∞ Analysis of Output Synchronization of Networked Dynamical Systems

Concepts like stability, performance, and robustness, which play a vital role in the analysis of networked dynamical systems (NDS), crucially depend on the network topology and subsystems (agents) dynamics, see, e.g., [118]. Hence, analysis of different topology structures and their influence on the robustness of the system is an important topic in the current research of NDS. In the NDS design, one may want to remove or add communication/sensing links in order to obtain favorable cooperative behaviors. Related analyses were carried out for other systems which have connections to NDS, such as vibrational systems [112, 130], as well as in other disciplines, such as social networks, health care systems and smart grids [113, 114, 126, 143].

This chapter discusses a numerically efficient approach for computing the maximal/minimal impact a subset of agents has on the whole networked dynamical system. For instance, if one is able to disturb/bolster several agents and wishes to maximally disturb/bolster the entire system, which agents should be chosen, and what kind of inputs should be applied? One way to quantify the impact of the chosen subset of agents to the system is to calculate the H_∞ norm of the mapping "exogenous disturbance of the chosen agents" $\mapsto$ "output of the system". For simplicity, the following discussion considers linear second-order agent dynamics and weighted undirected topologies where all agents share the same dynamical properties (i.e., homogeneous systems).

Works relating the H_∞ norm and NDS typically focus on syntheses [128, 138]. For example, the authors in [128] provide sufficient and necessary conditions for decentralized H_∞ and H_2 control design over directed graphs employing the algebraic Riccati equation or direct eigenstructure assignment. The analysis of NDS with respect to the performance of its agents is an area which seems to be under-researched. For instance, the analysis of networked dynamical systems in the general setting is missing. In particular, the efficient H_∞ norm calculation could be considered from the reduced order model perspective in the general system parameters. Moreover, the analysis of the H_2 norm in this context should be established and compared with the corresponding results obtained with the H_∞ norm.

Problem statement

Let F be a function in the space

$$\mathrm{H}_\infty = \Big\{ F \colon \mathbb{C}^+ \to \mathbb{C}^{m\times \ell} \;\Big|\; F \text{ analytic s.t. } \sup_{\lambda\in\mathbb{C}^+} \overline{\sigma}(F(\lambda)) < \infty \Big\},$$

where $\mathbb{C}^+ = \{\lambda \in \mathbb{C} \mid \Re(\lambda) > 0\}$ and $\overline{\sigma}(\cdot)$ is the largest singular value of a matrix. Then the H_∞ norm of F is defined to be [145, Chap. 3]

$$\|F\|_\infty = \sup_{\lambda \in \mathbb{C}^+} \overline{\sigma}(F(\lambda)) = \sup_{\omega \in \mathbb{R}} \overline{\sigma}(F(\mathrm{i}\omega)).$$

Let $\mathcal{G} = (\mathcal{V}, \mathcal{E}, \{w_{jk}\}_{j,k=1}^n)$ be an undirected weighted graph, with $\mathcal{V} = \{v_1, \ldots, v_n\}$, $\mathcal{E} \subset \mathcal{V} \times \mathcal{V}$ and where $w_{jk} \geq 0$ are edge weights such that $w_{jk} = w_{kj}$ for all j, k and $w_{jk} > 0$ if and only if $(j,k) \in \mathcal{E}$. Let $\mathcal{E}_i$ denote the set of vertices adjacent to the vertex i, i.e. $\mathcal{E}_i = \{j \in \mathcal{V} : (i,j) \in \mathcal{E}\}$. For

Consider n linear agents, indexed by $\mathcal{V}$ and given by

$$\ddot{\chi}_i = -T_s \dot{\chi}_i + K_s \upsilon_i + \eta_i \omega_i, \qquad T_s, K_s > 0, \tag{3.1}$$

where $\chi_i \in \mathbb{R}$ is the state, $\upsilon_i \in \mathbb{R}$ is the input, $\omega_i \in \mathbb{R}$ is the exogenous disturbance of the i^{th} agent, $i \in \{1, \ldots, n\}$, and $\eta_i \in \mathbb{R}$ is the corresponding disturbance weight.

A widely utilized decentralized output-feedback protocol to achieve network synchronization [118] is

$$\upsilon_i = -K\widehat{C} \sum_{j \in \mathcal{E}_i} w_{ij} \left(\begin{bmatrix} \chi_i \\ \dot{\chi}_i \end{bmatrix} - \begin{bmatrix} \chi_j \\ \dot{\chi}_j \end{bmatrix} \right), \tag{3.2}$$

where $K > 0$ and $\widehat{C} = [c_1 \quad c_2]$ with $c_1, c_2 > 0$.

A standing assumption herein is that the underlying graph $\mathcal{G}$ is connected.

In order to generalise to scenarios in which the disturbances ω_i are not necessarily all independent, assume that among the exogenous disturbances $\{\omega_1, \ldots, \omega_n\}$ there are $k \in \{1, \ldots, n\}$ different ones $\{\omega_{i_1}, \ldots, \omega_{i_k}\}$ (e.g., the same ocean waves or wind gusts concurrently disturb several agents). Then $\begin{bmatrix} \omega_1 & \ldots & \omega_n \end{bmatrix}^\top = H \begin{bmatrix} \omega_{i_1} & \ldots & \omega_{i_k} \end{bmatrix}^\top$, where the matrix $H \in \mathbb{R}^{n \times k}$ is given by

$$H_{j\ell} = \begin{cases} 1, & \omega_j = \omega_{i_\ell} \\ 0, & \text{otherwise} \end{cases}, \quad j = 1, \ldots, n, \;\; \ell = 1, \ldots, k.$$

Let $E = \operatorname{diag}(\eta_1, \ldots, \eta_n) H \in \mathbb{R}^{n \times k}$ denote the corresponding disturbance matrix. Assume that $\eta_i \neq 0$ if $H_{ii} \neq 0$, i.e., if the i^{th} agent is disturbed, then the corresponding weight is not zero. This in particular implies that E is a full rank matrix.

Let L be the Laplacian of the graph $\mathcal{G}$ (see, e.g. [13, Section 4.2]). Then the closed-loop dynamics can be written as

$$\ddot{\chi} + \big(\underbrace{T_s}_{:=\beta} I_N + L \underbrace{K_s K c_2}_{:=\alpha} \big) \dot{\chi} + L \underbrace{K_s K c_1}_{:=\gamma} \chi = E\omega, \tag{3.3}$$

where $\chi := (\chi_1, \ldots, \chi_n)$ and $\omega := (\omega_{i_1}, \ldots, \omega_{i_k})$.

The protocol (3.2) seeks for agreement/consensus, regardless of where that agreement is obtained. In particular, the system is invariant to translations, owing to the fact that $[1, 1, \ldots, 1]^\top$ is an eigenvector of L with respect to zero eigenvalue. Hence, the system can be reduced to obtain the single point equilibrium 0. Performing the reduction outlined in [111] yields the following system

$$\begin{cases} \dot{x} = Ax + B\omega \\ y = Cx, \end{cases} \tag{3.4}$$

where

$$A = \begin{bmatrix} \mathbf{0}_{(n-1)\times(n-1)} & V^\top \\ -\gamma LV & -\beta I_n - \alpha L \end{bmatrix},$$
$$B = \begin{bmatrix} \mathbf{0}_{(n-1)\times k} \\ E \end{bmatrix}, \quad C = \begin{bmatrix} V & \mathbf{0}_{n\times n} \end{bmatrix}.$$

The columns of matrix $V \in \mathbb{R}^{n\times(n-1)}$ span the subspace $\{\mathbf{1}\}^\perp$, where $\mathbf{1} = [1 \quad \dots \quad 1]^\top$ and V satisfies $V^\top V = I$.

One can obtain the following expressions for the transfer function $F(s) = C(\mathrm{i}s - A)^{-1}B$ of the system (3.4):

$$F(0) = \frac{1}{\gamma} L^+ E, \tag{3.5}$$

where L^+ denotes the Moore–Penrose pseudoinverse of L, and for $s \neq 0$:

$$F(s) = \frac{1}{\gamma + \mathrm{i}s\alpha} V V^T (L - \mu(s) I_n)^{-1} E, \tag{3.6}$$

where

$$\mu(s) = \frac{s^2 - \mathrm{i}s\beta}{\gamma + \mathrm{i}s\alpha}.$$

Main results

While it is well known that the H_∞ property in the following theorem holds for positive systems [116], in [110] the authors extend this to systems which are not necessarily positive as outlined in the following theorem and corollary.

Theorem 3.1.1. *Suppose that $\gamma \leq \alpha\beta$ or that $\gamma > \alpha\beta$ and $\|L\| \leq \frac{\beta^2}{2(\gamma-\alpha\beta)}$. Then*

$$\|F\|_\infty = \overline{\sigma}(F(0)).$$

Corollary 3.1.2. *Suppose that $\gamma \leq \alpha\beta$ or that $\gamma > \alpha\beta$ and $\|L\| \leq \frac{\beta^2}{2(\gamma-\alpha\beta)}$. Then among all disturbance matrices $E \in \mathbb{R}^{n\times k}$ with $\overline{\sigma}(E) \leq 1$, the maximum*

$$\max_{\substack{E\colon E\in\mathbb{R}^{n\times k} \\ 1\leq k\leq n,\, \overline{\sigma}(E)\leq 1}} \overline{\sigma}(L^+ E)$$

is attained at $\mathbb{R}^{n\times 1} \ni E = v_2$, where v_2 is the (normalized) eigenvector of L corresponding to λ_2, so-called the Fiedler vector.

Theorem 3.1.1 implies that maximal response of the system is obtained for constant disturbances. Also, among all E's from Corollary 3.1.2, it is enough to excite each agent with a constant disturbance and weights η_i's given by the Fiedler vector.

When analyzing a NDS, the H_∞ norm needs to be calculated many times. For example, "ranking" the agents by sensitivity to exogenous disturbances requires calculating the H_∞ norm for each agent. Using Theorem 3.1.1, this can be achieved efficiently on a standard computer even for very large NDSs, up to hundreds of thousands of agents.

Chapter 4

Applications Related to Gas Transport

4.1 Gas Market Modelling

The European gas market is governed by rules that are agreed on by the European Union. In [72], the authors present a mathematical market model that takes into account this structure, where the technical system operator (TSO) offers certain transportation capacities that can be booked and later nominated within the previously chosen bookings by the traders. The TSO also fixes booking fees and defines an operational control of the gas pipeline system in order to deliver the gas according to the nominations. Since the gas flow is governed by a system of partial differential equations (PDEs), such equations are also involved in the model in order to realize this control structure.

While four-level gas market models have been discussed previously, e.g. in [121], [72] takes into account the (transient) physics of gas flow by describing it not by a stationary model but by the semilinear isothermal Euler equations, see [41]. This influences the structure of the overall model and its reduction to a single level problem, alongside the corresponding necessary optimality conditions. A specific challenge that arises in the coupling investigated in [72] is that the PDE model and associated objectives are continuous in time whereas the market model and its objectives are discrete in time. The authors of [72] present methods that allow for coupling objectives of the two different types.

It was shown in [121] that, under suitable assumptions, the specific structure of the optimization problems and their coupling in the presented model allow for the reduction of the four-level model to an aggregated bilevel problem. In the upper level, of the resultant bilevel model, the TSO optimizes social welfare and the efficient allocation of the gas while the traders determine their bookings and nominations in an optimization problem on the lower-level. This complexity-reduction of the market model is done in terms of the associated stationarity or Karush-Kuhn-Tucker (KKT) conditions.

The authors of [72] propose a different method for reducing the complexity of the levels two and three. They show that the Nash games of the market participants can be phrased as potential generalized Nash equilibrium problems of the particular structure investigated in [56]. The inherent structure of the players' objectives and constraints in such games allows them to be replaced by a single optimization problem by choosing the correct potential function and feasible sets.

A specific feature of the model considered in [72] is that there is no direct influence of the PDE dynamics on the decisions of the traders concerning their nominations and bookings. The solution of the PDE dynamics only influences the booking fees and the technical capacities, both of which are exogenous parameters from the perspective of the traders. Therefore the coupling between the PDE model and the finite Nash games is realized through booking fees and technical capacities only.

The authors of [72] also provide examples for the optimal control problem of the TSO. For example, one task of the TSO is to determine the set of possible bookings that can be transported through the network.

4.2 Data Assimilation for Gas Networks via Distributed and Nodal Observers

Many algorithms for solving control problems (of gas flow in pipe networks) rely on knowledge (or at least a high fidelity approximation) of the system state. However, it is not possible to measure the complete state at all points in the network. One solution to this problem is the use of data assimilation techniques, i.e. combining partial measurements with a suitable PDE model for gas transport, in order to estimate the system state.

The work [63] studies observer-based data assimilation for gas transport using distributed measurements of one state variable. The gas flow is described by the barotropic Euler equations (1.13). For this system an observer system is constructed into which the measurements are inserted through a source term of Luenberger-type, cf. [102]. This is similar to the Luenberger-observer for the shallow water equations investigated in [18], which however requires the kinetic description of the PDEs to define the observer. The analysis in [63] avoids this requirement, simplifying the definition and analysis of discretized versions of the observer.

For velocity measurements, the observer system investigated in [63] is given by

$$\begin{cases} \partial_t \widehat{\rho} + \partial_x \widehat{m} = 0, & x \in [0,\ell],\ t > 0 \\ \partial_t \widehat{m} + \partial_x \Big(\dfrac{\widehat{m}^2}{\widehat{\rho}} + p(\widehat{\rho}) \Big) = -\dfrac{\gamma}{\widehat{\rho}} |\widehat{m}| \widehat{m} + \mu \widehat{\rho}(v - \widehat{v}), & x \in [0,\ell],\ t > 0 \end{cases} \tag{4.1}$$

with "nudging parameter" $\mu > 0$. Here, quantities without $\widehat{\cdot}$ refer to the state of the original system whereas quantities with $\widehat{\cdot}$ denote the state of the observer. In the first part of [63], the existence of solutions to the system (4.1) is shown for initial and boundary data that satisfy suitable smallness and compatibility conditions. This existence result extends the result from [73] to more general coupling and boundary conditions and to the observer system. The main idea of the proof is to first transform the system into the form incorporating the Riemann invariants, then rewrite this as a system of integral equations along the characteristic curves, and lastly to make use of a fixed-point argument. The second part of [63] discusses the relation between observer and system states, showing that the observer converges exponentially to the system state for long times, if the velocity in both systems and the time derivative of the exact solution are sufficiently small. This is done by estimating the difference between the state of the observer system and the original system state in terms of relative energy, in a manner similar to [49, 50]. The relative energy is extended via the addition of a suitable functional in order to control the error with respect to the unmeasured variable. This idea is based on an extension of the energy that was used in [51], see also [146]. The convergence is first proved for a single pipe before being extended to star-shaped networks.

In contrast, [70] considers an observer system that is based on nodal measurements. Synchronization of observers is related to control problems for the difference system, see [74] and references therein for an overview on boundary control of one-dimensional hyperbolic systems. In [70], which is inspired by the prior work [68] on boundary stabilization of gas flow on star-shaped networks, the authors consider gas flow on general networks, modeling the gas flow by a semilinear model that is obtained by transforming the Euler equations (1.13) to the form incorporating Riemann invariants and then linearizing the advective part of the system. Measurements of the exact state are inserted into the observer system as boundary or nodal conditions. If both systems have sufficiently smooth and bounded solutions and if for each pipe there is at least one adjacent node where measurements are available, then the exponential convergence of the observer state towards the original system state is shown via an observability inequality. Extending this work to a setting where measurements are only available at boundary nodes is an objective of current research.

In [69], the nodal observer system and its analysis is extended to a quasilinear 3×3 system that allows for hydrogen blending into natural gas. In addition, the effect of measurement errors is investigated. Provided measurements are available at all nodes of the network and certain smallness conditions are satisfied, the observer state is shown to converge to the system state, up to a difference of the size of the measurement errors [69].

4.3 Feedback Stabilization for the p-System at a Junction

In the work in progress [29], the authors consider $N \in \mathbb{N} \setminus \{0\}$ rectilinear tubes, each one modeled by the real interval $I = (0, 1)$, exiting a junction, which is located at the position $x = 0$. For $\ell \in \{1, \dots, N\}$, the direction and section of the ℓ-th tube are described, respectively, by the direction and the norm of a vector $\nu_\ell \in \mathbb{R}^3 \setminus \{0\}$. All tubes are filled with the same compressible, inviscid and isentropic (or isothermal) fluid, and friction along the walls is neglected. Hence, the fluid dynamics can be modeled through N copies of the one-dimensional p-system in Eulerian coordinates:

$$\begin{cases} \partial_t \rho_\ell + \partial_x q_\ell = 0, & t > 0,\ x \in [0, 1), \\ \partial_t q_\ell + \partial_x \left(\frac{q_\ell^2}{\rho_\ell} + p\left(\rho_\ell\right) \right) = 0, & t > 0,\ x \in [0, 1), \quad \ell \in \{1, \dots, N\}. \\ \left(\rho_\ell, q_\ell\right)(0, x) = \left(\rho_{0,\ell}, q_{0,\ell}\right), & x \in (0, 1), \end{cases} \tag{4.2}$$

Here, t is time, and, along the ℓ-th tube, x is the abscissa, ρ_ℓ is the fluid density, and q_ℓ is its linear momentum density. The pressure law $p = p(\rho)$ is the same for all tubes; it plays the role of the equation of state of the fluid under consideration and is assumed to satisfy the following hypothesis:

$$p \in \mathrm{C}^2(\mathbb{R}^+, \mathbb{R}^+), \quad p' > 0, \quad p'' > 0.$$

The authors consider the concept of P-solutions (see [31, 32]): namely, weak solutions of (4.2) such that

1. mass is conserved at the junction;
2. the trace of the flow of the linear momentum (also called dynamic pressure), i.e.

$$P(\rho_\ell, q_\ell) = \frac{q_\ell^2}{\rho_\ell} + p(\rho_\ell),$$

   at the junction is the same for all tubes;
3. entropy may not decrease at the junction.

The analysis extends the ideas of [33] which restricted its consideration to considering systems with two strictly positive eigenvalues. Generalising to broader classes of systems introduces several technical difficulties in the context of this problem.

Chapter 5

Further Applications

5.1 Analysis, Numerics, and Parametrization of Cross-Diffusion with Reaction Models

Following the pioneering work of Keller and Segel in the 1970s [83], cross-diffusion models have attracted significant interest in biology, chemistry, and physics for simulating systems with multiple species (see e.g. [60]).

Reaction-cross-diffusion models have been investigated from various perspectives and linked to numerous applications. Although cross-diffusion is a widespread phenomenon in complex networks and plays an important role in modelling complex natural phenomena, it is frequently overlooked in the analysis of reaction-diffusion networks. Key ingredients developed for the study of cross-diffusion PDEs and for networks of dynamical systems can be extended and combined in order to study cross-diffusion on complex networks (see e.g. [90]).

The application of cross-diffusion to image problems is not as frequent as its application to population dynamics or chemotaxis. The particular case of complex diffusion has been considered in the literature [14, 64]. In particular, nonlinear complex diffusion has been shown to be a numerically well-conditioned technique with successful applications to image restoration (see e.g. [12, 14]).

Alongside developments in modeling, the associated theory has evolved in synergy with practical applications, leading to increased interest in this area in recent years. Despite the widespread use of cross-diffusion models across numerous fields and the substantial mathematical developments surrounding them, several challenging problems and crucial questions remain to be addressed.

Mathematical model

Cross-diffusion models are described by time-dependent PDEs of diffusion/reaction-diffusion type, where the diffusive component incorporates a nonlinear non-diagonal diffusion matrix. This formulation results in a strongly coupled system where the evolution of each dependent variable depends both on its own dynamics and on the others, as dictated by the diffusion matrix and the reaction terms.

In this context, the evolution of the function $\mathbf{u} = (u_1(\mathbf{x},t),\dots,u_n(\mathbf{x},t))^\intercal$ describing (concentrations of) n species (chemical, biological, or otherwise) at position $\mathbf{x} \in \Omega \subset \mathbb{R}^m$, $m \in \{1,2,3\}$ and time $t > 0$ is governed by the initial-boundary-value problem

$$\begin{cases} \dfrac{\partial u_i}{\partial t} = \nabla \cdot \left(\displaystyle\sum_{j=1}^{n} D_{ij}(\mathbf{u}) \nabla u_j \right) + f_i(\mathbf{u}), & i = 1,\dots,n,\ \mathbf{x} \in \Omega,\ t > 0, \\ \left(\displaystyle\sum_{j=1}^{n} D_{ij}(\mathbf{u}) \nabla u_j \right) \cdot \nu = 0, & i = 1,\dots,n,\ \mathbf{x} \in \partial\Omega,\ t > 0, \\ \mathbf{u}(\mathbf{x},t) = \mathbf{u}_0(\mathbf{x}), & \mathbf{x} \in \Omega,\ t = 0. \end{cases} \tag{5.1}$$

Here $D_{ij}(\mathbf{u})$ is the nonlinear diffusion coefficient relating the jth species gradient with the flux of the ith species.

The mathematical properties and well-posedness of the corresponding initial-boundary value problems for these systems depend strongly on the associated diffusion matrix. When this matrix is symmetric and uniformly positive definite, well-posedness results (including a maximum principle) hold by standard arguments [3, 4]. When the matrix is only uniformly positive definite, existence and uniqueness of weak solutions can be obtained ([7, 60]) via the Schauder fixed point theorem ([19]).

The stability properties of explicit, implicit and semiimplicit finite difference schemes for a general nonlinear complex reaction-diffusion equation are derived in [9], and the corresponding convergence properties discussed in [8]. The stability results are generalized to cross-diffusion with reaction equations in [12].

It is known that implicit schemes have better stability properties when compared to their explicit counterparts, enabling the use of larger time steps and a broader range of diffusion coefficients. However, those advantages come at the price of high computational cost. The work [100] discusses operator splitting schemes as one route to lowering the computational load.

Learning stable numerical models

In [12] the authors aim to discover an optimal cross-diffusion reaction system for image denoising. To this end the optimal coefficients and influence functions which define the cross-diffusion matrix are determined. This is achieved by turning the PDE into a learnable architecture. Then, a back-propagation technique is used in order to minimize a cost function related to the quality of the denoising process, while ensuring stability of the underlying numerical method during the learning procedure. The benefits of including the stability conditions in the learning algorithm are evident from the simulations. The methodology used in [12] for the model parametrization, which is based on solving a constrained optimization problem using back-propagation, can be transferred to a broad range of PDE models aiming at different applications.

5.2 Mathematical Modeling and Optimization of Stents

A stent is a small, usually metallic, mesh that is placed in a narrowed or closed part of a blood vessel to keep the vessel open to restore normal blood flow. A variety of stents exist on the market with differing structures, sizes, geometries, and mechanical properties. Designing stents to meet prescribed mechanical constraints is a very demanding task. Despite the widespread use of vascular stents, the optimal design of their geometric and mechanical properties lacks a rigorous mathematical approach. The main reason for this is the fact that stents are three-dimensional solids and so are usually computationally modeled using 3D approaches, see [45, 58, 93, 105, 119] and the references therein. Designing an optimization algorithm based on 3D stent simulations is exceedingly complicated, and often times leads to an algorithm that is computationally very expensive and requires a large memory. The authors of [66], [67] propose a novel one-dimensional mathematical model for a stent based on the one-dimensional curved rod model from [81]. This essentially treats the stent as a graph $\mathcal{N} = (\mathcal{V}, \mathcal{E})$, i.e. a union of stent struts, with additional mechanical properties.

Thus, the (mixed) weak formulation of the entire stent is obtained by adding up the (mixed) weak formulations of each stent strut/edge. This is done for the functions $\mathbf{u}_S \in V_s$ denoting the collection of displacement vectors of middle lines and infinitesimal rotations of

cross–sections of all struts and $\mathbf{p}_S := (\mathbf{p}^1, \dots, \mathbf{p}^{n_\mathcal{E}}, \alpha, \beta) \in Q_S$, where

$$V_S = \mathrm{H}^1(\mathcal{N}; \mathbb{R}^6), \qquad Q_S = \mathrm{L}^2(\mathcal{N}; \mathbb{R}^3) \times \mathbb{R}^3 \times \mathbb{R}^3 = \prod_{i=1}^{n_\mathcal{E}} \mathrm{L}^2(0, \ell_i; \mathbb{R}^3) \times \mathbb{R}^3 \times \mathbb{R}^3. \tag{5.2}$$

These functions are defined on the entire stent, and the state variables $\mathbf{u}_S$ are continuous at vertices (globally continuous and thus belong to H^1). The functions $\mathbf{p}_S$ play the role of Lagrange multipliers, enforcing the inextensibility and unshearability condition, and zero total translation and rotation (see below).

After multiplying the differential equations of each stent strut (edge in the graph) by the components of the test functions $\tilde{\mathbf{u}}_S$, and integrating them by parts, and after taking the equilibrium of contact forces and contact moments at vertices/junctions of the graph into account, the resulting mixed weak formulation can be written in terms of the bilinear forms $k_S : V_S \times V_S \to \mathbb{R}$ and $b_S : Q_S \times V_S \to \mathbb{R}$, where:

$$\begin{cases} k_S(\mathbf{u}_S, \tilde{\mathbf{u}}_S) = \displaystyle\sum_{i=1}^{n_\mathcal{E}} \int_0^{\ell_i} \mathbf{Q}^i \mathbf{H}^i (\mathbf{Q}^i)^T \partial_s \boldsymbol{\omega}^i \cdot \partial_s \tilde{\boldsymbol{\omega}}^i ds, \\ b_S(\mathbf{p}_S, \tilde{\mathbf{u}}_S) = \displaystyle\sum_{i=1}^{n_\mathcal{E}} \int_0^{\ell_i} \mathbf{p}^i \cdot (\partial_s \tilde{\mathbf{u}}^i + \mathbf{t}^i \times \tilde{\boldsymbol{\omega}}^i) ds + \alpha \cdot \sum_{i=1}^{n_\mathcal{E}} \int_0^{\ell_i} \tilde{\mathbf{u}}^i ds + \beta \cdot \sum_{i=1}^{n_\mathcal{E}} \int_0^{\ell_i} \tilde{\boldsymbol{\omega}}^i ds. \end{cases} \tag{5.3}$$

Here $n_\mathcal{E}$ is the number of edges in the graph, ℓ_i is the length of the ith edge, $\mathbf{Q}^i$ denotes the local frame associated to the ith edge, $\mathbf{H}^i$ is a matrix that carries the information about properties of the material the stent is made of and the properties of the cross–sections of the stent struts. To deal with the forces, the following linear functional is introduced:

$$l_S : V_S \to \mathbb{R}, \qquad l_S(\tilde{\mathbf{u}}_S) = \sum_{i=1}^{n_\mathcal{E}} \int_0^{\ell_i} \mathbf{f}^i \cdot \tilde{\mathbf{u}}^i ds. \tag{5.4}$$

The *mixed formulation* of the state problem can then be stated as:

Find $(\mathbf{u}_S, \mathbf{p}_S) \in V_S \times Q_S$ such that

$$\begin{cases} k_S(\mathbf{u}_S, \tilde{\mathbf{u}}_S) + b_S(\mathbf{p}_S, \tilde{\mathbf{u}}_S) = l_S(\tilde{\mathbf{u}}_S), \quad \forall \tilde{\mathbf{u}}_S \in V_S, \\ b_S(\tilde{\mathbf{p}}_S, \mathbf{u}_S) = 0, \qquad \forall \tilde{\mathbf{p}}_S \in Q_S. \end{cases} \tag{5.5}$$

This model is in the mixed formulation, hence suitable for the finite element method (FEM). It is derived in detail in [66], where the existence of a unique solution is proven. The convergence of the FEM for it is proven in [67].

Numerically solving the model enables very efficient simulations that can lead to insights about the global properties of the stent without producing it, leading to questions of optimality. Optimization of the stent's strut thicknesses is done in [131], while the optimization of the geometry of struts is carried out in [132]. In both of these optimization problems the most typical cost function is the stent's overall compliance. To find a stent with minimal compliance, one seeks to minimize the elastic energy of the stent $k_S(\mathbf{u}_S, \mathbf{u}_S)$ in such a way that the resulting displacement, for a given outside forcing, satisfies the stent problem (5.5). Since the elastic energy for a given forcing must be equal $\int_\mathcal{N} \mathbf{f} \cdot \mathbf{u}_S ds$, inserting $\tilde{\mathbf{u}}_S = \mathbf{u}_S$ in the first equation in (5.5), leads to the following cost function $J : V_S \times Q_S \to \mathbb{R}$ for the problem of optimizing the overall stent's compliance:

$$J(\mathbf{u}_S, \mathbf{p}_S) = \int_\mathcal{N} \mathbf{f} \cdot \mathbf{u}_S ds = \sum_{i=1}^{n_\mathcal{E}} \int_0^{\ell^i} \mathbf{f}^i \cdot \mathbf{u}^i ds, \tag{5.6}$$

where $(\mathbf{u}_S, \mathbf{p}_S)$ is the solution of (5.5). Let $\mathbf{h}$ denote the finite set of parameters of optimization. In the stent's strut thicknesses optimization this is a vector with $n_{\mathcal{E}}$ thicknesses and in the geometry optimization with $n_{\mathcal{V}}$ scalars representing longitudinal position of the stent vertices. For a given value $\mathbf{h}$, let $(\mathbf{u}_S(\mathbf{h}), \mathbf{p}_S(\mathbf{h}))$ denote the solution of (5.5). The *optimal stent design problem* now reads as follows:

Find $\mathbf{h}^*$ such that

$$\begin{cases} J(\mathbf{u}_S(\mathbf{h}^*), \mathbf{p}_S(\mathbf{h}^*)) = \min\limits_{\mathbf{h}\in W} J(\mathbf{u}_S(\mathbf{h}), \mathbf{p}_S(\mathbf{h})), \\ \text{where } (\mathbf{u}_S(\mathbf{h}), \mathbf{p}_S(\mathbf{h})) \text{ is the unique solution of (5.5)}, \end{cases} \tag{5.7}$$

where $J(\mathbf{u}_S(\mathbf{h}), \mathbf{p}_S(\mathbf{h}))$ is given by (5.6).

The set W contains constraints, such as, e.g., the minimal and maximal value of parameters and a constraint on the total volume V_0 of the material the stent is made of for the thickness optimization problem.

Unlike the current data based approaches to optimization of 3D elastic structures [127, 129], in both cases it can be rigorously proven that the constrained optimization algorithm has a solution, and one can construct approximate solutions using the extremely efficient gradient descent method.

Affiliations

1. CMUC, Department of Mathematics, University of Coimbra, Apartado 3008, EC Santa Cruz, 3001-501 Coimbra, Portugal.
2. Alfréd Rényi Institute of Mathematics, Reáltanoda utca 13–15., 1053 Budapest, Hungary.
3. Department of Applied Analysis and Computational Mathematics, ELTE Eötvös Loránd University and HUN-REN-ELTE Numerical Analysis and Large Networks Research Group, Pázmány Péter sétány 1/C, 1117 Budapest, Hungary.
4. Bergische Universität Wuppertal, Gaußstrasse 20, 42119 Wuppertal, Germany.
5. Technical University of Darmstadt, Department of Mathematics, Dolivostr. 15, 64293 Darmstadt, Germany.
6. Lehrstuhl für Dynamics, Control, Machine Learning and Numerics (Alexander von Humboldt-Professur), Department Mathematik, Friedrich-Alexander-Universität Erlangen-Nürnberg, Cauerstr. 11, 91058 Erlangen, Germany.
7. Department of Differential Equations, Oles Honchar Dnipro National University, Gagarin av., 72 49010 Dnipro, Ukraine.
8. Department of Mathematics, Faculty of Science, University of Zagreb, Bijenicka 30, 10000 Zagreb, Croatia.
9. Faculty of Organization and Informatics, University of Zagreb, Croatia.
10. School of Applied Mathematics and Informatics, J. J. Strossmayer University of Osijek, Trg Ljudevita Gaja 6, Osijek, Croatia.
11. Institute of Applied Mathematics, Middle East Technical University, 06800, Ankara, Türkiye.
12. Departamento de Matemáticas, Universidad Autónoma de Madrid, 28049 Madrid, Spain.
13. Chair of Computational Mathematics, Fundación Deusto. Av. de las Universidades, 24, 48007 Bilbao, Basque Country, Spain.

Bibliography

[1] M. Akramov, J. Yusupov, M. Ehrhardt, H. Susanto, and D. Matrasulov. Transparent boundary conditions for the nonlocal nonlinear Schrödinger equation: A model for reflectionless propagation of PT-symmetric solitons. *Phys. Lett. A*, 459:128611, 2023.

[2] S. M. Allen and J. W. Cahn. A microscopic theory for antiphase boundary motion and its application to antiphase domain coarsening. *Acta Metall.*, 27:1159–1180, 1979.

[3] H. Amann. Dynamic theory of quasilinear parabolic systems. III. Global existence. *Math. Z.*, 202(2):219–250, 1989.

[4] B. Andreianov, M. Bendahmane, and R. Ruiz-Baier. Analysis of a finite volume method for a cross-diffusion model in population dynamics. *Math. Models Methods Appl. Sci.*, 21(2):307–344, 2011.

[5] B. Andreianov, G. M. Coclite, and C. Donadello. Well-posedness for vanishing viscosity solutions of scalar conservation laws on a network. *Discrete Contin. Dyn. Syst.*, 37(11):5913–5942, 2017.

[6] X. Antoine, E. Lorin, and Q. Tang. A friendly review of absorbing boundary conditions and perfectly matched layers for classical and relativistic quantum waves equations. *Molecular Phys.*, 115(15-16):1861–1879, 2017.

[7] A. Araújo, S. Barbeiro, E. Cuesta, and A. Durán. Cross-diffusion systems for image processing: II. The nonlinear case. *J. Math. Imaging Vision*, 58(3):427–446, 2017.

[8] A. Araújo, S. Barbeiro, and P. Serranho. Convergence of finite difference schemes for nonlinear complex reaction-diffusion processes. *SIAM J. Numer. Anal.*, 53(1):228–250, 2015.

[9] A. Araújo, S. Barbeiro, and P. Serranho. Stability of finite difference schemes for nonlinear complex reaction-diffusion processes. *IMA J. Numer. Anal.*, 35(3):1381–1401, 2015.

[10] A. Arnold. Numerically absorbing boundary conditions for quantum evolution equations. *VLSI Des.*, 6:313–319, 1998.

[11] J. Asier Bárcena-Petisco, M. Cavalcante, G. M. Coclite, N. de Nitti, and E. Zuazua. Control of hyperbolic and parabolic equations on networks and singular limits. Preprint: hal-03233211, 2021.

[12] S. Barbeiro and D. Lobo. Learning stable nonlinear cross-diffusion models for image restoration. *J. Math. Imaging Vision*, 62(2):223–237, 2020.

[13] L. W. Beineke and R. J. Wilson, editors. *Topics in structural graph theory*, volume 147 of *Encycl. Math. Appl.* Cambridge: Cambridge University Press, 2013.

[14] R. Bernardes, C. Maduro, P. Serranho, A. Araújo, S. Barbeiro, and J. Cunha-Vaz. Improved adaptive complex diffusion despeckling filter. *Opt. Express*, 18(23):24048–59, 2010.

[15] G. Bouchitté and I. Fragalà. Homogenization of thin structures by two-scale method with respect to measures. *SIAM J. Math. Anal.*, 32(6):1198–1226, 2001.

[16] G. Bouchitté and I. Fragalà. Homogenization of elastic thin structures: a measure-fattening approach. *J. Convex Anal.*, 9(2):339–362, 2002. Special issue on optimization (Montpellier, 2000).

[17] G. Bouchitté, I. Fragalà, and M. Rajesh. Homogenization of second order energies on periodic thin structures. *Calc. Var. Partial Differential Equations*, 20(2):175–211, 2004.

[18] A.-C. Boulanger, P. Moireau, B. Perthame, and J. Sainte-Marie. Data assimilation for hyperbolic conservation laws: a Luenberger observer approach based on a kinetic description. *Commun. Math. Sci.*, 13(3):587–622, 2015.

[19] H. Brezis. *Functional analysis, Sobolev spaces and partial differential equations*. Universitext. Springer, New York, 2011.

[20] J. Brouwer, I. Gasser, and M. Herty. Gas pipeline models revisited: model hierarchies, nonisothermal models, and simulations of networks. *Multiscale Model. Simul.*, 9(2):601–623, 2011.

[21] F. L. Cardoso-Ribeiro, D. Matignon, and L. Lefèvre. A partitioned finite element method for power-preserving discretization of open systems of conservation laws. *IMA J. Math. Control Inform.*, 38(2):493–533, 2021.

[22] J. A. Carrillo, S. Jin, and Y. Tang. Random batch particle methods for the homogeneous Landau equation. *Commun. Comput. Phys.*, 31(4):997–1019, 2022.

[23] V. Casarino, K.-J. Engel, R. Nagel, and G. Nickel. A semigroup approach to boundary feedback systems. *Integral Equations Oper. Theory*, 47(3):289–306, 2003.

[24] M. Cavalcante, G. M. Coclite, and N. De Nitti. Zero diffusion-dispersion limit for the Benjamin–Bona–Mahony–Burgers equation at a junction. Work in progress.

[25] Y. Chen, L. Lu, G. E. Karniadakis, and L. D. Negro. Physics-informed neural networks for inverse problems in nano-optics and metamaterials. *Opt. Express*, 28(8):11618, 2020.

[26] R. Chiheb, D. Cioranescu, A. El Janati, and G. Panasenko. Structures réticulées renforcées en élasticité [(French) Elasticity-enhanced reticulated structures]. *C. R. Acad. Sci. Paris Sér. I Math.*, 326(7):897–902, 1998.

[27] D. Cioranescu, A. Damlamian, and G. Griso. *The periodic unfolding method*, volume 3 of *Series in Contemporary Mathematics*. Springer, Singapore, 2018. Theory and applications to partial differential problems.

[28] D. Cioranescu and J. Saint Jean Paulin. *Homogenization of reticulated structures*, volume 136 of *Appl. Math. Sci.* Springer-Verlag, New York, 1999.

[29] G. M. Coclite, N. De Nitti, M. Garavello, F. Marcellini, and E. Zuazua. Feedback stabilization for entropy solutions of a 2×2 hyperbolic system of conservation laws at a junction. Work in progress.

[30] G. M. Coclite and M. Garavello. Vanishing viscosity for traffic on networks. *SIAM J. Math. Anal.*, 42(4):1761–1783, 2010.

[31] R. M. Colombo and M. Garavello. On the Cauchy problem for the p-system at a junction. *SIAM J. Math. Anal.*, 39(5):1456–1471, 2008.

[32] R. M. Colombo and M. Garavello. Comparison among different notions of solution for the p-system at a junction. *Discrete Contin. Dyn. Syst.*, 2009(Special):181–190, 2009.

[33] J.-M. Coron, S. Ervedoza, S. S. Ghoshal, O. Glass, and V. Perrollaz. Dissipative boundary conditions for 2×2 hyperbolic systems of conservation laws for entropy solutions in BV. *J. Differential Equations*, 262(1):1–30, 2017.

[34] J.-M. Coron and S. Guerrero. Singular optimal control: a linear 1-D parabolic-hyperbolic example. *Asymptot. Anal.*, 44(3-4):237–257, 2005.

[35] P. Csomós, M. Ehrhardt, and B. Farkas. Operator splitting for abstract Cauchy problems with dynamical boundary conditions. *Oper. Matrices*, 15(3):903–935, 2021.

[36] P. Csomós, B. Farkas, and B. Kovács. Error estimates for a splitting integrator for abstract semilinear boundary coupled systems. *IMA J. Numer. Anal.*, 43(6):3628–3655, 2023.

[37] N. De Nitti and E. Zuazua. On the controllability of entropy solutions of scalar conservation laws at a junction via Lyapunov methods. *Vietnam J. Math.*, 51(1):71–88, 2023.

[38] P. Degond and M. Tang. All speed scheme for the low Mach number limit of the isentropic Euler equations. *Commun. Comput. Phys.*, 10(1):1–31, 2011.

[39] W. Desch, I. Lasiecka, and W. Schappacher. Feedback boundary control problems for linear semigroups. *Isr. J. Math.*, 51:177–207, 1985.

[40] W. Desch, J. Milota, and W. Schappacher. Least square control problems in nonreflexive spaces. *Semigroup Forum*, 62(3):337–357, 2001.

[41] P. Domschke, J. Giesselmann, J. Lang, T. Breiten, V. Mehrmann, R. Morandin, B. Hiller, and C. Tischendorf. Gas Network Modeling: An Overview (Extended English Version). Technical report, available at: https://opus4.kobv.de/opus4-trr154/files/543/ModelCatalogue2023-DGLBMMHT.pdf, 2023.

[42] C. Donadello and V. Perrollaz. Exact controllability to trajectories for entropy solutions to scalar conservation laws in several space dimensions. *C. R. Math. Acad. Sci. Paris*, 357(3):263–271, 2019.

[43] B. Dorn, M. Kramar Fijavž, R. Nagel, and A. Radl. The semigroup approach to transport processes in networks. *Physica D*, 239(15):1416–1421, 2010.

[44] T. A. Driscoll, N. Hale, and L. N. Trefethen. *Chebfun Guide*. Pafnuty Publications, 2014.

[45] C. Dumoulin and B. Cochelin. Mechanical behaviour modelling of balloon-expandable stents. *J. Biomech.*, 33(11):1461–1470, 2000.

[46] W. E and B. Yu. The deep Ritz method: A deep learning-based numerical algorithm for solving variational problems. *Commun. Math. Stat.*, 6:1–12, 2018.

[47] H. Egger. A robust conservative mixed finite element method for isentropic compressible flow on pipe networks. *SIAM J. Sci. Comput.*, 40(1):A108–A129, 2018.

[48] H. Egger. Structure preserving approximation of dissipative evolution problems. *Numer. Math.*, 143(1):85–106, 2019.

[49] H. Egger and J. Giesselmann. Stability and asymptotic analysis for instationary gas transport via relative energy estimates. *Numer. Math.*, 153(4):701–728, 2023.

[50] H. Egger, J. Giesselmann, T. Kunkel, and N. Philippi. An asymptotic-preserving discretization scheme for gas transport in pipe networks. *IMA J. Numer. Anal.*, 43(4):2137–2168, 2023.

[51] H. Egger and T. Kugler. Damped wave systems on networks: exponential stability and uniform approximations. *Numer. Math.*, 138(4):839–867, 2018.

[52] H. Egger and N. Philippi. On the transport limit of singularly perturbed convection-diffusion problems on networks. *Math. Methods Appl. Sci.*, 44(6):5005–5020, 2021.

[53] A. El Janati. Asymptotic analysis of lattice-type plates depending on several small parameters. *Rev. Roumaine Math. Pures Appl.*, 43(9-10):819–838, 1998.

[54] K.-J. Engel and G. Fragnelli. Analyticity of semigroups generated by operators with generalized Wentzell boundary conditions. *Adv. Differ. Equ.*, 10(11):1301–1320, 2005.

[55] K.-J. Engel, M. Kramar Fijavž, R. Nagel, and E. Sikolya. Vertex control of flows in networks. *Netw. Heterog. Media*, 3(4):709–722, 2008.

[56] F. Facchinei, V. Piccialli, and M. Sciandrone. Decomposition algorithms for generalized potential games. *Comput. Optim. Appl.*, 50(2):237–262, 2011.

[57] U. S. Fjordholm, M. Musch, and N. H. Risebro. Well-posedness and convergence of a finite volume method for conservation laws on networks. *SIAM J. Numer. Anal.*, 60(2):606–630, 2022.

[58] A. Frank, P. Walsh, and J. Moore Jr. Computational fluid dynamics and stent design. *Artificial Organs*, 26(7):614–621, 2002.

[59] A. V. Fursikov and O. Y. Imanuvilov. *Controllability of evolution equations*, volume 34 of *Lecture Notes Ser.* Seoul National University, Research Institute of Mathematics, Global Analysis Research Center, Seoul, 1996.

[60] G. Galiano, M. L. Garzón, and A. Jüngel. Semi-discretization in time and numerical convergence of solutions of a nonlinear cross-diffusion population model. *Numer. Math.*, 93(4):655–673, 2003.

[61] Y. Geng, Y. Teng, Z. Wang, and L. Ju. A deep learning method for the dynamics of classic and conservative Allen-Cahn equations based on fully-discrete operators. *J. Comput. Phys.*, 496:112589, 2024.

[62] T. Geveci. On the application of mixed finite element methods to the wave equations. *RAIRO Modél. Math. Anal. Numér.*, 22(2):243–250, 1988.

[63] J. Giesselmann, M. Gugat, and T. Kunkel. Observer-based data assimilation for barotropic gas transport using distributed measurements. Preprint: arXiv:2303.04045, 2023.

[64] G. Gilboa, N. Sochen, and Y. Zeevi. Image enhancement and denoising by complex diffusion processes. *IEEE Trans. Pattern Anal. Mach. Intell.*, 26(8):1020–1036, 2004.

[65] G. Griso, L. Khilkova, J. Orlik, and O. Sivak. Homogenization of perforated elastic structures. *J. Elasticity*, 141(2):181–225, 2020.

[66] L. Grubišić, J. Iveković, J. Tambača, and B. Žugec. Mixed formulation of the one-dimensional equilibrium model for elastic stents. *Rad Hrvat. Akad. Znan. Umjet. Mat. Znan.*, 21(532):219–240, 2017.

[67] L. Grubišić and J. Tambača. Direct solution method for the equilibrium problem for elastic stents. *Numer. Linear Algebra Appl.*, 26(3):e2231, 23, 2019.

[68] M. Gugat and J. Giesselmann. Boundary feedback stabilization of a semilinear model for the flow in star-shaped gas networks. *ESAIM Control Optim. Calc. Var.*, 27:Paper No. 67, 24, 2021.

[69] M. Gugat and J. Giesselmann. An observer for pipeline flow with hydrogen blending in gas networks: exponential synchronization. Preprint: arXiv:2304.07375, 2023.

[70] M. Gugat, J. Giesselmann, and T. Kunkel. Exponential synchronization of a nodal observer for a semilinear model for the flow in gas networks. *IMA J. Math. Control Inform.*, 38(4):1109–1147, 2021.

[71] M. Gugat, X. Huang, and Z. Wang. Limits of stabilization of a networked hyperbolic system with a circle. *Control Cybernet.*, 52(1):79–121, 2023.

[72] M. Gugat, M. Schuster, and S. Steffensen. A Dynamic Multilevel Model of the European Gas Market. *Comm. Opt. Theory*, 11:1–26, 2023.

[73] M. Gugat and S. Ulbrich. Lipschitz solutions of initial boundary value problems for balance laws. *Math. Models Methods Appl. Sci.*, 28(5):921–951, 2018.

[74] A. Hayat. Boundary stabilization of 1D hyperbolic systems. *Annu. Rev. Control*, 52:222–242, 2021.

[75] M. Hernández and E. Zuazua. Random Batch Methods for PDE control on graphs. Work in progress.

[76] L. I. Ignat, A. F. Pazoto, and L. Rosier. Inverse problem for the heat equation and the Schrödinger equation on a tree. *Inverse Problems*, 28(1):015011, 30, 2012.

[77] A. D. Jagtap and G. E. Karniadakis. Extended physics-informed neural networks (XPINNs): A generalized space-time domain decomposition based deep learning framework for nonlinear partial differential equations. *Commun. Comput. Phys.*, 28(5):2002–2041, 2020.

[78] S. Jin, L. Li, and J.-G. Liu. Convergence of the random batch method for interacting particles with disparate species and weights. *SIAM J. Numer. Anal.*, 59(2):746–768, 2021.

[79] S. Jin, L. Li, X. Ye, and Z. Zhou. Ergodicity and long-time behavior of the Random Batch Method for interacting particle systems. *Math. Models Methods Appl. Sci.*, 33(1):67–102, 2023.

[80] P. Joly. Variational methods for time-dependent wave propagation problems. In *Topics in computational wave propagation*, volume 31 of *Lect. Notes Comput. Sci. Eng.*, pages 201–264. Springer, Berlin, 2003.

[81] M. Jurak and J. Tambača. Linear curved rod model. General curve. *Math. Models Methods Appl. Sci.*, 11(7):1237–1252, 2001.

[82] S. Karumuri, R. Tripathy, I. Bilionis, and J. Panchal. Simulator-free solution of high-dimensional stochastic elliptic partial differential equations using deep neural networks. *J. Comput. Phys.*, 404:109120, 2020.

[83] E. F. Keller and L. A. Segel. Initiation of slime mold aggregation viewed as an instability. *J. Theoret. Biol.*, 26(3):399–415, 1970.

[84] D. Ko and E. Zuazua. Model predictive control with random batch methods for a guiding problem. *Math. Models Methods Appl. Sci.*, 31(8):1569–1592, 2021.

[85] P. Kogut, O. Kupenko, and G. Leugering. Well-posedness and boundary observability of strongly degenerate hyperbolic systems on star-shaped planar network. *Pure Appl. Funct. Anal.*, 7(5):1767–1796, 2022.

[86] B. Kovács and C. Lubich. Numerical analysis of parabolic problems with dynamic boundary conditions. *IMA J. Numer. Anal.*, 37(1):1–39, 2017.

[87] M. Kramar and E. Sikolya. Spectral properties and asymptotic periodicity of flows in networks. *Math. Z.*, 249(1):139–162, 2005.

[88] M. Kramar Fijavž, D. Mugnolo, and E. Sikolya. Variational and semigroup methods for waves and diffusion in networks. *Appl. Math. Optim.*, 55(2):219–240, 2007.

[89] A. Krizhevsky, I. Sutskever, and G. Hinton. Imagenet classification with deep convolutional neural networks. In F. Pereira, C. J. C. Burges, L. Bottou, and K. Q.Weinberger, editors, *Advances in Neural Information Processing Systems 25*, pages 1097–1105. Curran Associates, Inc., 2012.

[90] C. Kuehn and C. Soresina. Cross-diffusion induced instability on networks. *J. Complex Netw.*, 12(2):Paper No. cnad052, 2024.

[91] M. Kütük and H. Yücel. A physics informed neural network preserving energy dissipation of Allen-Cahn equations. Work in progress.

[92] B. M. Lake, R. Salakhutdinov, and J. B. Tenenbaum. Human-level concept learning through probabilistic program induction. *Science*, 350:1332–1338, 2015.

[93] J. Lau. A stent is not just a stent: stent construction and design do matter in its clinical performance. *Singapore Med. J.*, 45(7):305–312, 2004.

[94] A. Lavrukhine, A. Popov, and I. Popov. On transparent vertex boundary conditions for quantum graphs. *Indian J. Phys.*, 97(7):2095–2102, 2023.

[95] Y. Liao and P. Ming. Deep Nitsche method: Deep Ritz method with essential boundary conditions. *Commun. Comput. Phys.*, 29:1365–1384, 2021.

[96] B. Liljegren-Sailer and N. Marheineke. On port-Hamiltonian approximation of a nonlinear flow problem on networks. *SIAM J. Sci. Comput.*, 44(3):B834–B859, 2022.

[97] J.-L. Lions. *Contrôlabilité exacte, perturbations et stabilisation de systèmes distribués. Tome 2, Perturbations. [(French) Exact controllability, perturbations and stabilization of distributed systems. Vol. 2, Perturbations.]*, volume 9 of *Rech. Math. Appl.* Masson, Paris, 1988.

[98] M. Ljulj, K. Schmidt, A. Semin, and J. Tambača. Homogenization of the planar one-dimensional periodic elastic rod structures, flexural case. Work in progress.

[99] M. Ljulj, K. Schmidt, A. Semin, and J. Tambača. Homogenization of the time-dependent heat equation on planar one-dimensional periodic structures. *Appl. Anal.*, 101(12):4046–4075, 2022.

[100] D. Lobo. Fast stable finite difference schemes for nonlinear cross-diffusion. *Comput. Math. Appl.*, 101:23–37, 2021.

[101] L. Lu, R. Pestourie, W. Yao, Z. Wang, F. Verdugo, and S. G. Johnson. Physics-informed neural networks with hard constraints for inverse design. *SIAM J. Sci. Comput.*, 43(6):B1105–B1132, 2021.

[102] D. Luenberger. An introduction to observers. *IEEE Trans. Automat. Control*, 16(6):596–602, 1971.

[103] Z. Mao, A. D. Jagtap, and G. E. Karniadakis. Physics-informed neural networks for high-speed flows. *Comput. Methods Appl. Mech. Engrg.*, 360:112789, 2020.

[104] R. Mattey and S. Ghosh. A novel sequential method to train physics informed neural networks for Allen Cahn and Cahn Hilliard equations. *Comput. Methods Appl. Mech. Eng.*, 390:114474, 2022.

[105] F. Migliavacca, L. Petrini, M. Colombo, F. Auricchio, and R. Pietrabissa. Mechanical behavior of coronary stents investigated through the finite element method. *J. Biomech.*, 35(6):803–811, 2002.

[106] A. G. Morgan. A mass-conserving formulation of the Generalized Benjamin-Bona-Mahony-Burgers equation on star networks. Preprint: arXiv:2103.03907, 2021.

[107] D. Mugnolo. *Semigroup methods for evolution equations on networks*. Underst. Complex Syst. Cham: Springer, 2014.

[108] D. Mugnolo and S. Romanelli. Dynamic and generalized Wentzell node conditions for network equations. *Math. Methods Appl. Sci.*, 30(6):681–706, 2007.

[109] M. Musch, U. S. Fjordholm, and N. H. Risebro. Well-posedness theory for nonlinear scalar conservation laws on networks. *Netw. Heterog. Media*, 17(1):101–128, 2022.

[110] I. Nakić, D. Tolić, I. Palunko, and Z. Tomljanović. Numerically efficient agents-to-group H_∞ analysis. *IFAC-PapersOnLine*, 55(20):199–204, 2022.

[111] I. Nakić, D. Tolić, I. Palunko, and Z. Tomljanović. Numerically efficient H_∞ analysis of cooperative multi-agent systems. *J. Franklin Inst.*, 359:9110–9128, 2022.

[112] I. Nakić, Z. Tomljanović, and N. Truhar. Mixed control of vibrational systems. *J. Appl. Math. Mech.*, 99(9):1–15, 2019.

[113] S. Peng, Y. Zhou, L. Cao, S. Yu, J. Niu, and W. Jia. Influence analysis in social networks: A survey. *J. Netw. Comput. Appl.*, 106:17–32, 2018.

[114] A. V. Proskurnikov and R. Tempo. A tutorial on modeling and analysis of dynamic social networks. Part I. *Annu. Rev. Control*, 43:65–79, 2017.

[115] M. Raissi, P. Perdikaris, and G. E. Karniadakis. Physics–informed neural networks: A deep learning framework for solving forward and inverse problems involving nonlinear partial differential equations. *J. Comput. Phys.*, 378:689–707, 2019.

[116] A. Rantzer. Scalable control of positive systems. *Eur. J. Control*, 24:72–80, 2015.

[117] G. A. Reigstad. Existence and uniqueness of solutions to the generalized Riemann problem for isentropic flow. *SIAM J. Appl. Math.*, 75(2):679–702, 2015.

[118] W. Ren and R. W. Beard. *Distributed Consensus in Multi-Vehicle Cooperative Control - Theory and Applications*. Communications and Control Engineering. Springer London, 2008.

[119] J. Russ, R. Li, A. Herschman, H. Waisman, V. Vedula, J. Kysar, and D. Kalfa. Design optimization of a cardiovascular stent with application to a balloon expandable prosthetic heart valve. *Mater. Des.*, 209:no. 109997, pp. 20, 2021.

[120] K. Sabirov, J. Yusupov, M. Aripov, M. Ehrhardt, and D. Matrasulov. Reflectionless propagation of Manakov solitons on a line: A model based on the concept of transparent boundary conditions. *Phys. Rev. E*, 103(4):043305, 2021.

[121] L. Schewe, M. Schmidt, and J. Thürauf. Global optimization for the multilevel European gas market system with nonlinear flow models on trees. *J. Glob. Optim.*, 82(3):627–653, 2022.

[122] M. E. Schonbek. Convergence of solutions to nonlinear dispersive equations. *Comm. Partial Differential Equations*, 7(8):959–1000, 1982.

[123] E. Sikolya. Flows in networks with dynamic ramification nodes. *J. Evol. Equ.*, 5(3):441–463, 2005.

[124] A. Singh and R. K. Sinha. Multioutput FOSLS deep neural network for solving Allen–Cahn equation. *Math. Models Comput. Simul.*, 15:1132–1146, 2023.

[125] J. Sirignano and K. Spiliopoulos. DGM: A deep learning algorithm for solving partial differential equations. *J. Comput. Phys.*, 375:1339–1364, 2018.

[126] F. Sorrentino, D. Tolić, R. Fierro, S. Picozzi, J. R. Gordon, and A. Mammoli. Stability analysis of a model for the market dynamics of a smart grid. In *52nd IEEE Conference on Decision and Control*, pages 4964–4970, 2013.

[127] I. Sosnovik and I. Oseledets. Neural networks for topology optimization. *Russian J. Numer. Anal. Math. Modelling*, 34(4):215–223, 2019.

[128] A. A. Stoorvogel, A. Saberi, M. Zhang, and Z. Liu. Solvability conditions and design for H_∞ & H_2 almost state synchronization of homogeneous multi-agent systems. *Eur. J. Control*, 46:36–48, 2019.

[129] M. Tezzele, F. Ballarin, and G. Rozza. Combined parameter and model reduction of cardiovascular problems by means of active subspaces and POD-Galerkin methods. In *Mathematical and numerical modeling of the cardiovascular system and applications*, volume 16 of *SEMA SIMAI Springer Ser.*, pages 185–207. Springer, Cham, 2018.

[130] Z. Tomljanović and M. Voigt. Semi-active $\mathcal{H}_\infty$-norm damping optimization by adaptive interpolation. *Numer. Linear Algebra Appl.*, 27(4):1–17, 2020.

[131] S. Čanić, L. Grubišić, D. Lacmanović, M. Ljulj, and J. Tambača. Optimal design of vascular stents using a network of 1D slender curved rods. *Comput. Methods Appl. Mech. Engrg.*, 394:Paper No. 114853, 32, 2022.

[132] S. Čanić, L. Grubišić, M. Ljulj, M. Maretić, and J. Tambača. Geometric optimization of vascular stents modeled as networks of 1D rods. *J. Comput. Phys.*, 494:Paper No. 112497, 32, 2023.

[133] D. W. M. Veldman, A. Borkowski, and E. Zuazua. Stability and convergence of a randomized model predictive control strategy. *IEEE Trans. Autom. Control*, pages 1–8, 2024.

[134] D. W. M. Veldman and E. Zuazua. A framework for randomized time-splitting in linear-quadratic optimal control. *Numer. Math.*, 151(2):495–549, 2022.

[135] A. D. Wentzell. On boundary conditions for multidimensional diffusion processes. *Theory Probab. Appl.*, 4:164–177, 1960.

[136] C. L. Wight and J. Zhao. Solving Allen–Cahn and Cahn–Hilliard equations using the adaptive physics informed neural networks. *Commun. Comput. Phys.*, 29:930–954, 2021.

[137] H. Xu, J. Chen, and F. Ma. Adaptive deep learning approximation for Allen–Cahn equation. In D. Groen, C. de Mulatier, M. Paszynski, V. V. Krzhizhanovskaya, J. J. Dongarra, and P. M. A. Sloot, editors, *Computational Science – ICCS 2022*, pages 271–283, Cham, 2022. Springer International Publishing.

[138] F. A. Yaghmaie, K. H. Movrić, F. L. Lewis, and R. Su. Differential graphical games for H_∞ control of linear heterogeneous multiagent systems. *Internat. J. Robust Nonlinear Control*, 29(10):2995–3013, 2019.

[139] J. Yusupov, K. Sabirov, Q. Asadov, M. Ehrhardt, and D. Matrasulov. Dirac particles in transparent quantum graphs: Tunable transport of relativistic quasiparticles in branched structures. *Phys. Rev. E*, 101(6):062208, 2020.

[140] J. Yusupov, K. Sabirov, M. Ehrhardt, and D. Matrasulov. Transparent nonlinear networks. *Phys. Rev. E*, 100(3):032204, 2019.

[141] J. Yusupov, K. Sabirov, M. Ehrhardt, and D. Matrasulov. Transparent quantum graphs. *Phys. Lett. A*, 383(20):2382–2388, 2019.

[142] J. R. Yusupov, M. Ehrhardt, K. S. Matyokubov, and D. U. Matrasulov. Driven transparent quantum graphs. Preprint: arXiv:2312.01448, 2023.

[143] B. Zhao, Y. K. Li, J. C. S. Lui, and D. M. Chiu. Mathematical modeling of advertisement and influence spread in social networks. In *ACM Workshop on the Economics of Networked Systems (NetEcon)*, 2009.

[144] V. V. Zhikov. Averaging of problems in the theory of elasticity on singular structures. *Izv. Ross. Akad. Nauk Ser. Mat.*, 66(2):81–148, 2002.

[145] K. Zhou, J. C. Doyle, and K. K Glover. *Robust and Optimal Control*. Prentice Hall, Upper Saddle River, NJ, 1996.

[146] E. Zuazua. Stability and decay for a class of nonlinear hyperbolic problems. *Asymptotic Anal.*, 1(2):161–185, 1988.